Balancing discretization and numerical error for coupled parabolic hyperbolic problems using the dual weigthed residual method with application to thermoelasticity

Andreas Rademacher

Andreas.Rademacher@tu-dortmund.de, Chair of Scientific Computing, Technische Universität Dortmund, Vogelpothsweg 87, 44227 Dortmund

Abstract

In this article, we consider coupled parabolic hyperbolic problems, as they arise in thermoelasticity. Starting from a space time finite element discretization, a goal oriented a posteriori error estimated based on the dual weighted residual (DWR) method is derived, which measures the discretization error in space and time as well as the numerical error, where the splitting of the spatial and temporal error is based only on the properties of the used patchwise higher order reconstruction. We present an adaptive strategy, which balances the spatial and temporal discretization error as well as the numerical error. Finally, some numerical examples substantiate the efficiency of our approach.

Keywords: coupled parabolic hyperbolic problems, adaptive finite element method, dual weighted residual method

1 Introduction

In many engineering problems, the interdependency of mechanical quantities like the stresses and the temperature plays a dominant role. One example is the deep hole drilling process with minimum quantity lubrication (MQL), where the drilling process on the one hand induces heat into the workpiece and on the other hand due to the resulting thermal stresses large workpiece deviations occur, which can lead to the total failure of the process. A detailed description of this process, of its macroscopic modelling, and of an efficient finite element simulation can be found in [8]. One key question in designing a solution approach for such coupled models is to rate the strength of the coupling between the mechanical and the thermal part. For instance in [8], it is shown that the coupling is very weak such that the solution of the mechanical and the thermal part can completely be decoupled saving a large amount of computation time. The aim of this article is to develop a methodology, where the strength of the coupling is automatically measured and the solution process is adaptively adapted.

The presented approach relies on a posteriori error control especially the dual weighted residual (DWR) method. For a general overwiev of the DWR method, we refer to [4, 6], where also a first approach to error control concerning the discretization of the heat as well as the wave equation

is included. An enhanced method for nonlinear parabolic problems is presented in [31] and applied on optimal control problems with nonlinear parabolic constraints in [24]. This ansatz is extended to nonlinear hyperbolic problems of second order in [26]. The adaptive optimal control of such a type of problem is discussed in [18]. The estimates significantly simplify for quasi-periodic solution, cf. [10, 12], where model adaptive algorithms are also considered. A different linearization is used in [32] to derive the error identity. Beside the DWR approach, there exist a lot of other methods for a posteriori error estimation in literature. For an overview concerning parabolic problems, we refer to the textbook [35], where also first convergence results are discussed. Adaptive methods for hyperbolic problems of second order are rarely studied in literature. One approach, which is used to estimate the error in global norms, is based on finite difference discretisations in time. Here, separate error estimators are used for the space and the time direction [9, 20, 36] or error estimates for the whole problem are derived [1, 7]. The other approach, which is used here, is based on a space-time Galerkin method. Discontinuous Galerkin schemes are the basis for the error estimators presented in [2, 15, 19]. There, the norm of the error in the last time step is controlled, where the dual solution is estimated by analytical arguments and not solved numerically. The same approach for a continuous space-time Galerkin method is presented in [14]. Several results concerning goal-oriented adaptive finite element methods for structural dynamics are published by the group of Schweizerhoff [16, 17, 21, 25]. An important topic of their work is the reduction of the numerical effort of the error estimation, which is also considered in [34]. Coupled parabolic hyperbolic problems are, e. g., considered in [2, 33].

The approach to a posteriori error control of the discretization error used in this article is an extension of the methods presented [26, 31] to coupled parabolic hyperbolic problems. It is based on a space-time finite element discretization of the underlying problem. Since we have an hyperbolic part in our system, we use globally continuous ansatz functions in space and time while the test functions can be discontinuous in time. This approach ensures energy conservation under suitable assumptions, see for instance [26, Proposition 1.2.7]. Using apropriate quadrature rules, it corresponds to a Crank-Nicolson scheme of second order. In every time step, a coupled problem in the displacement and in the temperature has to be solved, where a staggered solution sheme is used, i. e. a fixpoint iteration consisting in alternately solving w. r. t. the displacement and the temperature. We apply the general framework of the DWR method for estimating the discretization error in some user defined target functional, cf. e. g. [6], on this space-time setting, which gives rise to a so called dual problem and a special dual time stepping scheme, which does not coincide with the Crank-Nicolson scheme. As usual in DWR methods, we have to calculate higher order approximations of the primal and dual solution to approximate the analytic error identity. Several approaches are known in literature, see [4] for an overview. Here, we use a patchwise reconstruction of higher order, since this approach is numerically cheap and allows for a splitting of the spatial and the temporal error. Measuring the strength of the coupling corresponds to estimating the error in the staggered solution scheme. To this end, we adopt the techniques presented in [23, 27, 28] for measuring the numerical error in the DWR method considering static problems. Roughly speaking, the numerical error correlate to the primal residual tested with the dual solution. The information of the error estimator is used in an adaptive strategy to balance the numerical, spatial and temporal error.

The article is organized as follows: In Section 2, some notation and the underlying analytical problem setting is introduced. Followed by a description of the space time finite element discretization in Section 3, where the resulting time stepping scheme is presented in the appendix, Section A. The main part of the paper is Section 4, where the a posteriori error estimate is derived in several steps. First of all, the analytic error identity involving the primal and dual

residual plus a remainder term is proven, see Section 4.1. The error identity involves the analytic and discrete dual problem, which are discussed in detail in Section 4.2. The corresponding dual time stepping scheme is outlined in the appendix, Section B. The error identity involves the analytic primal and dual solution. Thus it cannot be evaluated directly. We introduce a numerical approximation scheme in Section 4.3, which also allows us to split the spatial and temporal error. Finally, the error estimate is localized to the single mesh cells in Section 4.4, where the concrete terms are given in the appendix, Section C. The error estimator is utilized in the adaptive algorithm discussed in Section 5 and outlined in detail in the appendix, Section D. To illustrate the properties of our adaptive ansatz, we discuss several numerical examples considering linear and nonlinear thermoelasticity in Section 6. In the end, we draw some conclusions and present an outlook to further open questions.

2 Problem setting

In this section, we present the underlying general problem formulation having in mind thermoelastic problems. Some concrete examples are discussed in Section 6. At first, some notation is introduced. Let $\Omega \subset \mathbb{R}^d$, $d = 1, 2, 3$, be a bounded domain with a piecewise polygonal boundary Γ. The boundary Γ is decomposed in the mutually disjoint parts Γ_D and Γ_N. The basic function spaces are given by $L^2(\Omega)$, which provided the scalar product $(u, v) = \int_\Omega uv\, dx$ is a Hilbert space, and $\mathcal{L}^2(\Omega) = \left(L^2(\Omega)\right)^d$. Furthermore, we use the Sobolev space $H^1(\Omega)$, which consists of all functions in $L^2(\Omega)$ that possess first weak derivatives also in $L^2(\Omega)$, its subspace $H^1_D(\Omega) = \left\{v \in H^1(\Omega) \,\middle|\, v_{|\Gamma_D} = 0\right\}$, where $v_{|\Gamma_D}$ denotes the trace of v on Γ_D, and $\mathcal{H}^1_D(\Omega) := \left(H^1_D(\Omega)\right)^d$. Dual spaces are generally marked by a * and the dual pairing is denoted by $\langle\cdot,\cdot\rangle$. To study Sobolev spaces involving time, we use the Bochner integral theory. Here, X is a real Banach space with norm $\|\cdot\|$. The space $L^2(I; X)$ consists of all strongly measureable functions $\varphi : I \to X$ with

$$\|\varphi\|_{L^2(I;X)} := \left(\int_I \|\varphi\|^2 \, dt\right)^{1/2} < \infty,$$

where $I = [0, T]$ denotes a time interval. Weak derivatives w.r.t. time are marked by superposed dots. If X is a Hilbert space, the space-time scalar product is denoted by $((u, v)) := \int_I (u, v)\, dt$. In general, an outer parenthesis denotes the integration over I. Finally, we define the basic function space, which contain our weak solution, by

$$\begin{aligned} V_1 &:= \left\{ u \in L^2\left(I; \mathcal{H}^1_D(\Omega)\right) \,\middle|\, \begin{array}{l} \dot{u} \in L^2\left(I; \mathcal{L}^2(\Omega)\right), \\ \ddot{u} \in L^2\left(I; \left(\mathcal{H}^1_D(\Omega)\right)^\star\right) \end{array} \right\}, \\ V_2 &:= \left\{ \theta \in L^2\left(I; H^1_D(\Omega)\right) \,\middle|\, \dot{\theta} \in L^2\left(I; \left(H^1_D(\Omega)\right)^\star\right) \right\}. \end{aligned}$$

It should be remarked that $u \in C\left(I; \mathcal{H}^1_D(\Omega)\right)$ and $\dot{u} \in C\left(I; \mathcal{L}^2(\Omega)\right)$ holds for a function $u \in V_1$ as well as $\theta \in C\left(I; L^2(\Omega)\right)$ for $\theta \in V_2$.

Now, we are able to define a weak solution of our general problem:

Definition 1. We say the displacement $u \in V_1$ and the temperature $\theta \in V_2$ are a weak solution of our general coupled parabolic hyperbolic problem, if

$$b_1(\ddot{u}, \chi) + a_1(u; \theta)(\chi) = l_1(\chi) \tag{1}$$

$$b_2\left(\dot{\theta}, \omega\right) + a_2(\theta; u)(\omega) = l_2(\omega) \tag{2}$$

holds for all $\chi \in \mathcal{H}^1_D(\Omega)$, all $\omega \in H^1_D(\Omega)$ and a. e. $t \in I$ as well as if the initial conditions

$$u(0) = u_s, \quad \dot{u}(0) = v_s, \quad \theta(0) = \theta_s$$

are satisfied. Here, b_1 and b_2 denote weighted dual pairings. In our applications, the weights are specified by some physical constants like density. The semilinearforms a_1 and a_2 represent the differential operators of the elasticity equation and the heat equation respectively. The right hand sides are given by the linearforms l_1 and l_2. Finally, we have the initial values $u_s \in \mathcal{H}^1_D(\Omega)$, $v_s \in \mathcal{L}^2(\Omega)$, and $\theta_s \in H^1_D(\Omega)$.

The basis of our discretization is a space-time formulation of the general coupled parabolic hyperbolic problem. To this end, we rewrite (1) as a system of first order in time by introducing the velocity $v = \dot{u}$ as additional variable, where the equality is only weakly enforced. The equations (1) and (2) are integrated over the time interval I and the initial conditions are weakly included. To ease notation, we use

$$\mathcal{V}^n := \left\{ v \in L^2\left(I; \left(H^1_D(\Omega)\right)^n\right) \middle| \dot{v} \in L^2\left(I; \left(L^2(\Omega)\right)^n\right) \right\}$$

as the basic function space with $n = 1, 2, 3$, which imposes somewhat stronger assumptions on the solution than V_1 and V_2. Finally, the space-time formulation reads:

Definition 2. A function $w = (u, v, \theta) \in V = \mathcal{V}^d \times \mathcal{V}^d \times \mathcal{V}^1$ is called a weak solution of our general coupled parabolic hyperbolic problem in space time form, if

$$A(w)(\varphi) = 0$$

holds for all $\varphi = (\chi, \psi, \omega) \in V$ with

$$\begin{aligned} A(w)(\varphi) \quad := \quad & (b_1(\dot{u} - v, \psi)) + (b_1(\dot{v}, \chi)) + (a_1(u; \theta)(\chi)) - (l_1(\chi)) \\ & + \left(b_2\left(\dot{\theta}, \omega\right)\right) + (a_2(\theta; u)(\omega)) - (l_2(\omega)) \\ & + b_1(u(0) - u_s, \psi(0)) + b_1(v(0) - v_s, \chi(0)) + b_2(\theta(0) - \theta_s, \omega(0)). \end{aligned}$$

Due to the stronger assumptions in V, b_1 and b_2 can be seen as weighted L^2-scalar products here.

In our general setting, the question of existence and uniqueness of the solution w has to be left open. For our discretization and a posteriori error analysis, we assume that the space time semilinearform A is three times continuously Fréchet differentiable w. r. t. the first argument, that an isolated weak solution $w \in V$ according to Definition 2 exists, and that the Fréchet derivative of A leads to a well-posed linear problem in the neighbourhood of w.

3 Discretization

We use a space-time finite element method in this work. Let us start with the temporal part of the discretization. The time interval I is decomposed into $M \in \mathbb{N}$ subintervals $I_m = (t_{m-1}, t_m]$ with

$$0 = t_0 < t_1 < \ldots < t_M = T \quad \text{and} \quad I = \{0\} \cup I_1 \cup \ldots \cup I_M.$$

The length of a subinterval I_m is denoted by $k_m = t_m - t_{m-1}$. The time instances t_i, $i \in \{0, 1, \ldots, M\}$ correspond to the time steps in a finite difference approach. We also call this decomposition temporal mesh $\mathbb{T}_k$.

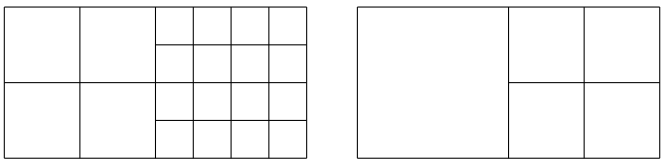

(a) Mesh with patch structure (b) Corresponding patch mesh

Fig. 1: Illustration of the patch structure of the finite element mesh

The spatial domain Ω is subdivided by meshes $\mathbb{T}_h^m$, which consist of quadrilaterals for $d = 2$ and of hexahedrons for $d = 3$. To realize adaptive mesh refinement, we allow for so called (spatial) hanging nodes in the meshes. Furthermore, for the evaluation of the presented a posteriori error estimate, we require the meshes to have patch structure, see Figure 1 for an illustration. Here, we say, roughly speaking, a mesh has patch structure, if one can always merge 2^d adjacent mesh elements to one patch element. We refer to [26] for more details. The sequence of meshes in the single time steps is called $\mathbb{M}_h := (\mathbb{T}_h^m)_{0 \le m \le M}$.

The spatial finite element spaces are based on d-linear basis functions and nodal degrees of freedom, i. e. we choose

$$V_h^m := \left\{ \varphi \in H_D^1(\Omega) \,\middle|\, \forall \mathcal{T} \in \mathbb{T}_h^m : \varphi_{|\mathcal{T}} \in Q_1(\mathcal{T}, \mathbb{R}) \right\}.$$

Here, $Q_1(\mathcal{T}, \mathbb{R})$ is the set of d-linear basis functions on a mesh element $\mathcal{T}$. Because of $V_h^m \subset C(\Omega)$, we have to ensure the continuity of the discrete functions in hanging nodes by imposing the resulting constraint in the discrete systems.

The test space of the space-time Galerkin method is given by

$$\mathcal{W}_{kh}^n := \left\{ \varphi \in L^2\left(I; \left(H_D^1(\Omega)\right)^n\right) \,\middle|\, \varphi_{|I_m} \in \mathcal{P}_0\left(I_m; (V_h^m)^n\right),\ m = 1, 2, \ldots, M,\ \varphi(0) \in \left(V_h^0\right)^n \right\}.$$

Here, $\mathcal{P}_q(\omega, X)$ is the linear space of polynomials on $\omega \subset \mathbb{R}$ with values in X, which have the maximum degree q. Functions from $\mathcal{W}_{kh}^n$ are piecewise constant in time and are possibly discontinuous at t_i, $i = 0, 1, \ldots, M$. The definition of the trial space $\mathcal{V}_{kh}^n$ is more involved, since it is difficult to ensure the global continuity, if the spaces V_h^m vary. Then hanging nodes in time arise and have to be treated in an appropriate way. A temporal hanging node is a degree of freedom, which is contained in V_h^m but not in V_h^{m-1} or vice versa. We work with the approach presented in [5, 22, 31] for parabolic problems. A discussion of hanging nodes in time in the context of the wave equation is given in [3]. We use linear temporal basis functions and choose the usual Lagrange basis of $\mathcal{P}_1(I_m; \mathbb{R})$

$$\tau_0^m(t) = \frac{t_m - t}{k_m} \quad \text{and} \quad \tau_1^m(t) = \frac{t - t_{m-1}}{k_m}.$$

We define the set of the local basis functions by

$$\tilde{\mathcal{P}}_1^{n,m} := \operatorname{span}\left\{ \tau_0^m \left(V_h^{m-1}\right)^n, \tau_1^m \left(V_h^m\right)^n \right\}.$$

The space $\tilde{\mathcal{P}}_1^{n,m}$ coincides with $\mathcal{P}_1(I_m; V_h^n)$, if $V_h^{m-1} = V_h^m = V_h$ holds. The trial space is given by

$$\mathcal{V}_{kh}^n := \left\{ \varphi_{kh} \in C\left(I; \left(H_D^1(\Omega)\right)^n\right) \,\middle|\, \varphi_{kh|I_m} \in \tilde{\mathcal{P}}_1^{n,m},\ m = 1, 2, \ldots, M \right\}.$$

Spatial basis functions from V_h^{m-1}, which vanish when stepping from t_{m-1} to t_m, are only connected to the temporal basis funtion τ_0, which is zero at t_m. Spatial basis functions from V_h^m, which arise when stepping from t_{m-1} to t_m, are only coupled with the temporal basis function τ_1 and τ_1 vanishes at t_{m-1}. Thus, all functions in V_{kh} are globally continuous. Using the above definitions, we state the discrete problem formulation:

Definition 3. A function $w_{kh} = (u_{kh}, v_{kh}, \theta_{kh}) \in V_{kh} = \mathcal{V}_{kh}^d \times \mathcal{V}_{kh}^d \times \mathcal{V}_{kh}^1$ is called a discrete solution of our general coupled parabolic hyperbolic problem, if

$$A\left(w_{kh}\right)\left(\varphi_{kh}\right) = 0 \tag{3}$$

holds for all $\varphi_{kh} = (\chi_{kh}, \psi_{kh}, \omega_{kh}) \in W_{kh} = \mathcal{W}_{kh}^d \times \mathcal{W}_{kh}^d \times \mathcal{W}_{kh}^1$.

The discrete problem (3) can directly be solved leading to a $d+1$ dimensional problem. However, the special structure of the test space W_{kh} allows for a decoupling of the single time intervals I_m. By this, the discrete problem (3) can be reduced to a time stepping scheme. However, we only compute an approximation $\tilde{w}_{kh}$ to w_{kh} resulting from the solution of the discrete coupled system here. For the evaluation of the time integrals, we use the trapezoidal rule. This approach results in a Crank-Nicolson method for the system of first order. For the hyperbolic part, it corresponds to Newmark's method. Furthermore, we can eliminate the velocity from the arising system in each time step. Thus, we only need to solve an nonlinear equation in the displacement $\tilde{u}_{kh}$ and the temperature $\tilde{\theta}_{kh}$. The complete time stepping scheme is outlined in Algorithm 9 in the appendix in Section A. In the first step, the discrete initial values a determined as L^2-projection of the continuous ones. We use a staggered solution scheme, which is given in the steps 3 to 7. Firstly, the solutions of the preceding time step are projected on the current mesh by $\mathbb{P}_h^m$. Here, we solve equation (13) w. r. t. the temperature $\tilde{\theta}_{kh}^{m,l}$ for fixed $\tilde{u}_{kh}^{m,l-1}$ first. Then the new displacement $\tilde{u}_{kh}^{m,l}$ is determined using $\tilde{\theta}_{kh}^{m,l}$ by solving equation (14). In step 6, we check the usual stopping criterion for a fixed point iteration. After the convergence of this iteration, the velocity $\tilde{v}_{kh}^m$ is calculated in the post processing step 8, where equation (15) corresponds to a simple L^2-projection, which reduces to a linear combination of vectors, if $V_h^{m-1} = V_h^m$ holds.

4 A posteriori error estimation

The aim is to derive an a posteriori error estimate for the discretisation error in a more or less arbitrary functional, which represents the quantity of interest. We consider functionals of the type

$$J(w) := \int_0^T J_1(w)\,dt + J_2(w(T)), \tag{4}$$

where J_1, $J_2 \in V^\star$ are three times continuously Fréchet differentiable. The form of J specified in (4) considers two typical situations: One is interested in the mean value of a quantity over I or in the value at the end point.

4.1 Derivation of the error identity

The derivation of the error estimate is based on optimization arguments. To embed the error estimation in the optimization context, we define the Lagrangian

$$\mathcal{L}(w, z) := J(w) - A(w)(z)$$

for $w, z \in V$. The connection between the Lagrangian and the general coupled parabolic hyperbolic problem becomes apparent as soon as we consider the Fréchet derivative of $\mathcal{L}$ w.r.t. z:

$$\mathcal{L}_z' (w, z) (\delta w, \delta z) = -A(w)(\delta z). \tag{5}$$

It corresponds to the weak formulation of the general coupled parabolic hyperbolic problem. In the discrete case, we recover the space-time Galerkin approximation. The Fréchet derivative w.r.t. w is

$$\mathcal{L}_w'(w, z)(\delta w, \delta z) = J'(w)(\delta w) - A'(w)(\delta w, z), \tag{6}$$

which defines the so called dual problem.

Definition 4. The function $z = \left(\bar{u}, \bar{v}, \bar{\theta}\right) \in V$ is called dual solution if

$$J'(w)(\delta w) - A'(w)(\delta w, z) = 0 \tag{7}$$

holds for all $\delta w \in W$. The discrete dual solution $z_{kh} = \left(\bar{u}_{kh}, \bar{v}_{kh}, \bar{\theta}_{kh}\right) \in W_{kh}$ is specified by

$$\forall \delta w_{kh} \in V_{kh} : \quad J' \left(w_{kh}\right) \left(\delta w_{kh}\right) - A' \left(w_{kh}\right) \left(\delta w_{kh}, z_{kh}\right) = 0. \tag{8}$$

We call its numerical approximation $\tilde{z}_{kh}$. The time stepping scheme for the determination of $\tilde{z}_{kh}$ is presented after the derivation of the a posteriori error estimate.

The point $(w, z) \in V \times V$ is a stationary point of $\mathcal{L}$, i.e.

$$\mathcal{L}'(w, z)(\delta w, \delta z) = 0 \tag{9}$$

for all $(\delta w, \delta z) \in V \times V$. Analogously, $(w_{kh}, z_{kh}) \in V_{kh} \times W_{kh}$ is a stationary point of $\mathcal{L}$, i.e.

$$\mathcal{L}' \left(w_{kh}, z_{kh}\right) \left(\delta w_{kh}, \delta z_{kh}\right) = 0 \tag{10}$$

for all $(\delta w_{kh}, \delta z_{kh}) \in W_{kh} \times V_{kh}$.

The following a posteriori error analysis is complicated by the facts that on the one hand in general

$$\mathcal{L}' \left(\tilde{w}_{kh}, \tilde{z}_{kh}\right) \left(\delta w_{kh}, \delta z_{kh}\right) \neq 0$$

and that on the other hand $W_{kh} \nsubseteq V$. We obtain the following result:

Proposition 5. *Let A and J be three times continuously Fréchet differentiable, the continuous stationarity condition (9) and discrete one (10) hold, as well as $\tilde{w}_{kh} \in V_{kh}$ and $\tilde{z}_{kh} \in W_{kh}$ are approximations of $w_{kh} \in V_{kh}$ and $z_{kh} \in W_{kh}$. Then we have the error identity*

$$\begin{aligned} & J(w) - J\left(\tilde{w}_{kh}\right) \\ =& \frac{1}{2} \mathcal{L}' \left(\tilde{w}_{kh}, \tilde{z}_{kh}\right) \left(w - \tilde{w}_{kh}, z - \tilde{z}_{kh}\right) + A\left(\tilde{w}_{kh}\right) \left(\tilde{z}_{kh}\right) + \mathcal{R}_{kh} \\ =& \frac{1}{2} \left[\rho \left(\tilde{w}_{kh}\right) \left(z - \tilde{z}_{kh}\right) + \rho^{\star} \left(\tilde{w}_{kh}, \tilde{z}_{kh}\right) \left(w - \tilde{w}_{kh}\right)\right] + A\left(\tilde{w}_{kh}\right) \left(\tilde{z}_{kh}\right) + \mathcal{R}_{kh}. \end{aligned} \tag{11}$$

Here, the primal residual ρ is given by

$$\rho \left(\tilde{w}_{kh}\right) (\cdot) := \mathcal{L}_z' \left(\tilde{w}_{kh}\right) (\cdot) = -A \left(\tilde{w}_{kh}\right) (\cdot)$$

and the dual residual $\rho^\star$ *by*

$$\rho^\star\left(\tilde{w}_{kh},\tilde{z}_{kh}\right)(\cdot) := \mathcal{L}'_w\left(\tilde{w}_{kh},\tilde{z}_{kh}\right)(\cdot) = J'\left(\tilde{w}_{kh}\right)(\cdot) - A'\left(\tilde{w}_{kh}\right)(\cdot,\tilde{z}_{kh}).$$

The remainder term

$$\begin{aligned}\mathcal{R}_{kh} \;:=\; & \frac{1}{2}\int_0^1 \left\{J'''\left(\tilde{w}_{kh}+s\tilde{e}\right)\left(\tilde{e},\tilde{e},\tilde{e}\right) - A'''\left(\tilde{w}_{kh}+s\tilde{e}\right)\left(\tilde{e},\tilde{e},\tilde{e},\tilde{z}_{kh}+s\tilde{e}^*\right)\right. \\ & \left. -3A''\left(\tilde{w}_{kh}+s\tilde{e}\right)\left(\tilde{e},\tilde{e},\tilde{e}^*\right)\right\} s\left(s-1\right)\,ds\end{aligned}$$

is of third order in the primal error $\tilde{e} := w - \tilde{w}_{kh}$ *and the dual error* $\tilde{e}^* := z - \tilde{z}_{kh}$.

Proof. Introducing the notation $x := (u,z)$, $\tilde{x}_{kh} := (\tilde{w}_{kh},\tilde{z}_{kh})$, and $L(x) := \mathcal{L}(u,z)$, we obtain

$$L(x) - L\left(\tilde{x}_{kh}\right) = \int_0^1 L'\left(\tilde{x}+s\left(x-\tilde{x}_{kh}\right)\right)\left(x-\tilde{x}_{kh}\right)\,ds.$$

For the trapezoidal rule, we have the error representation

$$\int_0^1 f(s)\,ds = \frac{1}{2}\left(f(0)+f(1)\right) + \frac{1}{2}\int_0^1 f''(s)\,s\left(s-1\right)\,ds$$

for $f \in C^2\left((0,1)\right)$. Bringing these two things together leads to

$$\begin{aligned}J(w) - J\left(\tilde{w}_{kh}\right) &= L(x) + A(w)(z) - L\left(\tilde{x}_{kh}\right) + A\left(\tilde{w}_{kh}\right)\left(\tilde{z}_{kh}\right) \\ &= \int_0^1 L'\left(\tilde{x}+s\left(x-\tilde{x}_{kh}\right)\right)\left(x-\tilde{x}_{kh}\right)\,ds + A\left(\tilde{w}_{kh}\right)\left(\tilde{z}_{kh}\right) \\ &= \frac{1}{2}\mathcal{L}'\left(\tilde{w}_{kh},\tilde{z}_{kh}\right)\left(w-\tilde{w}_{kh},z-\tilde{z}_{kh}\right) + \frac{1}{2}\mathcal{L}'\left(w,z\right)\left(w-\tilde{w}_{kh},z-\tilde{z}_{kh}\right) \\ &\quad + A\left(\tilde{w}_{kh}\right)\left(\tilde{z}_{kh}\right) + \mathcal{R}_{kh}.\end{aligned}$$

By a density argument, cf. [22, Theorem 6.2] for the parabolic and [26, Proposition 1.3.2] for the hyperbolic case, we can finally show that $\mathcal{L}'(w,z)\left(w-\tilde{w}_{kh},z-\tilde{z}_{kh}\right) = 0$ and therewith finish the proof. □

4.2 Dual problem

The error identity (11) involves the quantities z and $\tilde{z}_{kh}$, which are defined by the stationarity conditions (9) and (10) as solutions of the variational problems (7) and (8), respectively. These problems are called the continuous and the discrete dual problem, respectively. Let us now take a closer look at the continuous dual problem. The Fréchet derivative of A w.r.t. w is given by

$$\begin{aligned}A'(w)(\delta w,z) &= \left(b_1\left(\dot{\delta u}-\delta v,\bar{v}\right)\right) + \left(b_1\left(\dot{\delta v},\bar{u}\right)\right) + \left(a'_{1,u}\left(u;\theta\right)\left(\delta u,\bar{u}\right)\right) + \left(a'_{1,\theta}\left(u;\theta\right)\left(\delta\theta,\bar{u}\right)\right) \\ &\quad + \left(b_2\left(\dot{\delta\theta},\bar{\theta}\right)\right) + \left(a'_{2,\theta}\left(\theta;u\right)\left(\delta\theta,\bar{\theta}\right)\right) + \left(a'_{2,u}\left(\theta;u\right)\left(\delta u,\bar{\theta}\right)\right) \\ &\quad + b_1\left(\delta u(0),\bar{v}(0)\right) + b_1\left(\delta v(0),\bar{u}(0)\right) + b_2\left(\delta\theta(0),\bar{\theta}(0)\right).\end{aligned}$$

We use integration by parts to shift the time derivative from the test functions to the solution variables and obtain

$$\begin{aligned}A'(w)(\delta w,z) &= -\left(b_1\left(\delta v,\bar{v}+\dot{\bar{u}}\right)\right) - \left(b_1\left(\delta u,\dot{\bar{v}}\right)\right) + \left(a'_{1,u}\left(u;\theta\right)\left(\delta u,\bar{u}\right)\right) + \left(a'_{1,\theta}\left(u;\theta\right)\left(\delta\theta,\bar{u}\right)\right) \\ &\quad - \left(b_2\left(\delta\theta,\dot{\bar{\theta}}\right)\right) + \left(a'_{2,\theta}\left(\theta;u\right)\left(\delta\theta,\bar{\theta}\right)\right) + \left(a'_{2,u}\left(\theta;u\right)\left(\delta u,\bar{\theta}\right)\right) \\ &\quad + b_1\left(\delta u(T),\bar{v}(T)\right) + b_1\left(\delta v(T),\bar{u}(T)\right) + b_2\left(\delta\theta(T),\bar{\theta}(T)\right).\end{aligned}$$

The Fréchet derivative of J is

$$\begin{aligned} J'(w)(\delta w) &= J'_u(w)(\delta u) + J'_v(w)(\delta v) + J'_\theta(w)(\delta\theta) \\ &= \int_0^T J'_{1,u}(w)(\delta u)\,dt + J'_{2,u}(w(T))(\delta u(T)) \\ &\quad + \int_0^T J'_{1,v}(w)(\delta v)\,dt + J'_{2,v}(w(T))(\delta v(T)) \\ &\quad + \int_0^T J'_{1,\theta}(w)(\delta\theta)\,dt + J'_{2,\theta}(w(T))(\delta\theta(T)). \end{aligned}$$

Testing equation (7) with $\varphi_1 = (\delta u, 0, 0)$, $\varphi_2 = (0, \delta v, 0)$, and $\varphi_3 = (0, 0, \delta\theta)$ for arbitrary $\delta u \in \mathcal{V}^d$, $\delta v \in \mathcal{V}^d$, and $\delta\theta \in \mathcal{V}^1$, we obtain the system

$$\begin{aligned} -\left(b_1\left(\delta u, \dot{\bar{v}}\right)\right) + \left(a'_{1,u}\left(u;\theta\right)\left(\delta u, \bar{u}\right)\right) + \left(a'_{2,u}\left(\theta;u\right)\left(\delta u, \bar{\theta}\right)\right) + b_1\left(\delta u\left(T\right), \bar{v}\left(T\right)\right) &= J'_u(w)(\delta u), \\ -\left(b_1\left(\delta v, \bar{v} + \dot{\bar{u}}\right)\right) + b_1\left(\bar{u}(T), \delta v(T)\right) &= J'_v(w)(\delta v), \\ -\left(b_2\left(\delta\theta, \dot{\bar{\theta}}\right)\right) + \left(a'_{2,\theta}\left(\theta;u\right)\left(\delta\theta, \bar{\theta}\right)\right) + \left(a'_{1,\theta}\left(u;\theta\right)\left(\delta\theta, \bar{u}\right)\right) + b_2\left(\delta\theta\left(T\right), \bar{\theta}\left(T\right)\right) &= J'_\theta(w)(\delta\theta). \end{aligned}$$

This formulation provides more insight into the structure of the dual problem. The first important observation is that the dual problem starts at T and runs backward in time to 0. Consequently, the initial values are specified for T. Furthermore, the dual problem is linear. The homogeneous Dirichlet boundary conditions of the primal problem are transferred to the dual problem. The nonhomogeneous Neumann boundary conditions are transformed into homogeneous ones. The descriptive interpretation of the dual solution is that it represents the influence of a certain space-time point (x,t) onto the error measured in the functional J.

Let us now take a closer look at the discrete dual problem specified in equation (8). We observe that the discrete solution $\tilde{z}_{kh}$ is contained in the test space W_{kh} of the primal problem, i.e. $\tilde{z}_{kh}$ is a piecewise constant function in time. Thus, the approximation of the dual problem is globally of maximum order k. However, we are not interested in an accurate numerical solution of the dual problem but in an accurate a posteriori error estimate. The time stepping scheme resulting from (8) differs from the primal time stepping scheme described in Algorithm 10 in the appendix in Section B. For the derivation of the dual time stepping scheme from (8), we rewrite the Fréchet derivative by means of elementwise integration by parts and using $\dot{z}_{kh} \equiv 0$ as

$$\begin{aligned} A'\left(\tilde{w}_{kh}\right)\left(\delta w_{kh}, \tilde{z}_{kh}\right) &= \sum_{m=1}^{M} \left\{ -\left(b_1\left(\delta v_{kh}, \tilde{\bar{v}}_{kh}\right)\right)_m + \left(a'_{1,u}\left(\tilde{u}_{kh}; \tilde{\theta}_{kh}\right)\left(\delta u_{kh}, \tilde{\bar{u}}_{kh}\right)\right)_m \right\} \\ &\quad + \sum_{m=1}^{M} \left\{ \left(a'_{1,\theta}\left(\tilde{u}_{kh}; \tilde{\theta}_{kh}\right)\left(\delta\theta_{kh}, \tilde{\bar{\theta}}_{kh}\right)\right)_m - b_1\left(\left[\tilde{\bar{u}}_{kh}\right]_{m-1}, \delta v_{kh}^{m-1}\right) \right\} \\ &\quad + \sum_{m=1}^{M} \left\{ -b_1\left(\left[\tilde{\bar{v}}_{kh}\right]_{m-1}, \delta u_{kh}^{m-1}\right) + \left(a'_{2,\theta}\left(\tilde{\theta}_{kh}; \tilde{u}_{kh}\right)\left(\delta\theta_{kh}, \tilde{\bar{\theta}}_{kh}\right)\right)_m \right\} \\ &\quad + \sum_{m=1}^{M} \left\{ -b_2\left(\left[\tilde{\bar{\theta}}_{kh}\right]_{m-1}, \delta\theta_{kh}^{m-1}\right) + \left(a'_{2,u}\left(\tilde{\theta}_{kh}; \tilde{u}_{kh}\right)\left(\delta u_{kh}, \tilde{\bar{\theta}}_{kh}\right)\right)_m \right\} \\ &\quad + b_1\left(\delta v_{kh}^M, \tilde{\bar{u}}_{kh}^{M,-}\right) + b_1\left(\delta u_{kh}^M, \tilde{\bar{v}}_{kh}^{M,-}\right) + b_2\left(\delta\theta_{kh}^M, \tilde{\bar{\theta}}_{kh}^{M,-}\right). \end{aligned}$$

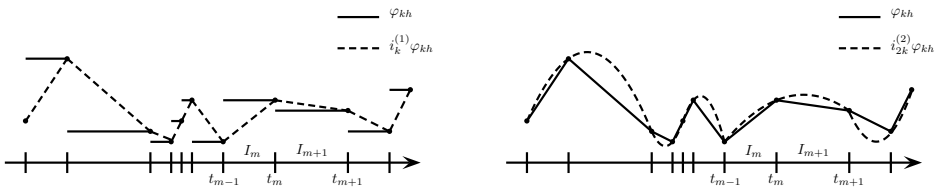

(a) Piecewise linear interpolation of a piecewise constant function

(b) Piecewise quadratic interpolation of a piecewise linear function

Fig. 2: Illustration of the interpolation operators $i_k^{(1)}$ and $i_{2k}^{(2)}$

Here, the jump of a possibly discontinuous function ω at a time instance t_m is defined by

$$\omega^{m,+} := \lim_{t \downarrow t_m} \omega(t), \quad ,\omega^{m,-} := \lim_{t \uparrow t_m} \omega(t), \quad [\omega]_m := \omega^{m,+} - \omega^{m,-}.$$

Using special test functions, we can now deduce the dual time stepping scheme. It is outlined in Algorithm 10 in the appendix in Section B and consists of solving two coupled Helmholtz equations and a simple L^2-projection.

4.3 Numerical approximation of the error identity and error splitting

We have discussed the numerical solution of the dual problem, which is needed to evaluate the error identity (11). However, the identity (11) contains the weights $w - \tilde{w}_{kh}$ and $z - \tilde{z}_{kh}$. The weights measure the approximation or interpolation error of the spaces V_{kh} and W_{kh} w.r.t. the continuous solutions w and z. We are not able to evaluate these terms exactly. In literature, many approaches to approximate these terms are proposed, see, e.g., [4] for an overview. The idea to use a higher order reconstruction of the discrete solutions $\tilde{w}_{kh}$ and $\tilde{z}_{kh}$ has turned out to be an accurate and efficient approximation. Thus, we also use this idea here. Furthermore, it allows us to split the spatial and the temporal part of the error, see Lemma 6.

In space, we need a higher order reconstruction of the d-linear basis functions. Consequently, we work with d-quadratic basis functions to define the reconstruction. For d-quadratic basis functions, which shall be based on nodal values, 3^d nodal values are needed to determine the basis coefficients. We use the patch structure of the spatial meshes to obtain these nodal values, see Figure 1 for an illustration. The function space, which contains the interpolating functions, is

$$V_{2h}^{(2),m} := \left\{ \varphi \in L^2(\Omega) \,\middle|\, \forall \mathcal{T} \in \mathbb{T}_{2h}^m : \varphi_{|\mathcal{T}} \in Q_2(\mathcal{T}; \mathbb{R}) \right\}, \tag{12}$$

where $\mathbb{T}_{2h}^m$ is the mesh of the patch elements in the m^{th}-time step and $Q_2(\mathcal{T}; \mathbb{R})$ is the space of the d-quadratic basis functions. Eventually, we obtain the operator $i_{2h}^{(2)} : V_h^m \to V_{2h}^{(2),m}$, which maps a finite element function from V_h^m into the space $V_{2h}^{(2),m}$. Furthermore, we define the projection $\Pi_{2h}^{(2)} := i_{2h}^{(2)} - \mathrm{id}$.

For the definition of the space time interpolations of higher order, we set $\mathcal{V}_{kh}^{(1,1)} := \mathcal{V}_{kh}$, $\mathcal{V}_{kh}^{(0,1)} := \mathcal{W}_{kh}$,

$$\mathcal{V}_{kh}^{(0,2)} := \left\{ \varphi_{kh} \in L^2\left(I; H_D^1(\Omega)\right) \,\middle|\, \begin{array}{c} \varphi_{kh|I_m} \in \mathcal{P}_0\left(I_m; V_{2h}^{(2),m}\right), \\ m = 1, \ldots, M,\ \varphi_{kh}(0) \in V_{2h}^{(2),0} \end{array} \right\}.$$

We set $\tau_0^{(1)} := \tau_0$ and $\tau_1^{(1)} := \tau_1$ the linear temporal basis functions on I_m. The quadratic temporal basis functions on $I_m \cup I_{m+1}$ are given by

$$\begin{aligned}
\tau_0^{(2)}(t) &:= \frac{(t_m - t)(t_{m+1} - t)}{k_m (k_m + k_{m+1})}, \\
\tau_1^{(2)}(t) &:= \frac{(t - t_{m-1})(t_{m+1} - t)}{k_m k_{m+1}}, \\
\tau_2^{(2)}(t) &:= \frac{(t - t_{m-1})(t - t_m)}{(k_m + k_{m+1}) k_{m+1}}.
\end{aligned}$$

Furthermore, we define

$$\begin{aligned}
\tilde{\mathcal{P}}_{1,2}^m &:= \left\{ \tau_i^{(1)} \varphi_i \,\middle|\, \varphi_i \in V_{2h}^{(2),m-1+i},\ i = 0,1 \right\}, \\
\tilde{\mathcal{P}}_{2,1}^m &:= \left\{ \tau_i^{(2)} \varphi_i \,\middle|\, \varphi_i \in V_h^{m-1+i},\ i = 0,1,2 \right\}, \\
\tilde{\mathcal{P}}_{2,2}^m &:= \left\{ \tau_i^{(2)} \varphi_i \,\middle|\, \varphi_i \in V_{2h}^{(2),m-1+i},\ i = 0,1,2 \right\}.
\end{aligned}$$

Finally, we denote

$$\mathcal{V}_{kh}^{(i,j)} := \left\{ \varphi_{kh} \in C\left(I; H_D^1(\Omega)\right) \,\middle|\, \varphi_{kh|I_m} \in \tilde{\mathcal{P}}_{i,j}^m,\ m = 1,2,\ldots,M \right\}$$

for $i,j = 1,2$. In time, we use the spatial interpolation operator of higher order $i_{2h}^{(2)}$ transferred to the one dimensional case for the interpolation of piecewise linear and continuous functions. The approach is illustrated in Figure 2(b). The interpolation is named $i_{2k}^{(2)}$. For the piecewise constant temporal basis functions, we specify a linear interpolant $i_k^{(1)}$. The idea is exemplified in Figure 2(a). We define the projections

$$\Pi_k^{(1)} := i_k^{(1)} - \mathrm{id} \text{ and } \Pi_{2k}^{(2)} := i_{2k}^{(2)} - \mathrm{id}$$

for the temporal interpolants.

Now, we are able to define our space-time reconstruction of higher order. For $i = 0,1,2$ and $j = 1,2$, let $\phi \in \mathcal{V}_{kh}^{(i,j)}$. The function ϕ can be represented by the temporal basis functions $\tau^{(i),m}$ in the form

$$\phi(x,t) = \sum_{m=0}^{M} \tau^{(i),m}(t) \cdot \varphi^m(x)$$

with $\varphi^m(x) \in V_h^m$. We define three different space-time interpolation operators: The first one only interpolates the spatial part and is given by

$$\begin{aligned}
i_h^{(j,2)} &: \mathcal{V}_{kh}^{(j,1)} \to \mathcal{V}_{kh}^{(j,2)}, \\
i_h^{(j,2)} \phi(x,t) &:= \sum_{m=0}^{M} \tau^{(j),m}(t) \cdot i_{2h}^{(2)} \varphi^m(x),
\end{aligned}$$

for $j = 0,1,2$. Let

$$\begin{aligned}
i_k^{(j+1,i)} &: \mathcal{V}_{kh}^{(j,i)} \to \mathcal{V}_{kh}^{(j+1,i)}, \\
i_k^{(j+1,i)} \phi(x,t) &:= \sum_{m=0}^{M} i_k^{(j+1)} \tau^{(j),m}(t) \cdot \varphi^m(x),
\end{aligned}$$

for $j = 0, 1$ and $i = 1, 2$ be the interpolation operator, which only interpolates the temporal part. The operator interpolating in space and time is

$$\begin{aligned} i_{hk}^{(j+1,2)} &: \mathcal{V}_{kh}^{(j,1)} \to \mathcal{V}_{kh}^{(j+1,2)}, \\ i_{kh}^{(j+1,2)}\phi(x,t) &:= \sum_{m=0}^{M} i_k^{(j+1)}\tau^{(j),m}(t) \cdot i_{2h}^{(2)}\varphi^m(x), \end{aligned}$$

for $j = 0, 1$. We are now able to define the space time projections. They are given by

$$\begin{array}{ll} \Pi_{2h}^{(j,2)} : \mathcal{V}_{kh}^{(j,1)} \to \mathcal{V}_{kh}^{(j,2)}, & \Pi_{2h}^{(j,2)} := i_h^{(j,2)} - \mathrm{id}, \quad j = 0, 1, 2, \\ \Pi_{k}^{(1,j)} : \mathcal{V}_{kh}^{(0,j)} \to \mathcal{V}_{kh}^{(0,j)} \cup \mathcal{V}_{kh}^{(1,j)}, & \Pi_{k}^{(1,j)} := i_k^{(1,j)} - \mathrm{id}, \quad j = 1, 2, \\ \Pi_{2k}^{(2,j)} : \mathcal{V}_{kh}^{(1,j)} \to \mathcal{V}_{kh}^{(2,j)}, & \Pi_{2k}^{(2,j)} := i_k^{(2,j)} - \mathrm{id}, \quad j = 1, 2, \\ \Pi_{k,2h}^{(1,2)} : \mathcal{V}_{kh}^{(0,1)} \to \mathcal{V}_{kh}^{(0,1)} \cup \mathcal{V}_{kh}^{(1,2)}, & \Pi_{k,2h}^{(1,2)} := i_{kh}^{(1,2)} - \mathrm{id}, \\ \Pi_{2k,2h}^{(2,2)} : \mathcal{V}_{kh}^{(1,1)} \to \mathcal{V}_{kh}^{(2,2)}, & \Pi_{2k,2h}^{(2,2)} := i_{kh}^{(2,2)} - \mathrm{id}. \end{array}$$

We have stated the higher order reconstruction for the scalar case to ease the notation here. They can directly be extended to vector valued functions. Now, we can state the approximation of the error identity (11):

$$\begin{aligned} & J(w) - J(\tilde{w}_{kh}) \\ = \; & \frac{1}{2}\left[\rho(\tilde{w}_{kh})(z - \tilde{z}_{kh}) + \rho^\star(\tilde{w}_{kh}, \tilde{z}_{kh})(w - \tilde{w}_{kh})\right] + A(\tilde{w}_{kh})(\tilde{z}_{kh}) + \mathcal{R}_{kh} \\ \approx \; & \frac{1}{2}\left[\rho(\tilde{w}_{kh})\left(\Pi_{k,2h}^{(1,2)}\tilde{z}_{kh}\right) + \rho^\star(\tilde{w}_{kh}, \tilde{z}_{kh})\left(\Pi_{2k,2h}^{(2,2)}\tilde{w}_{kh}\right)\right] + A(\tilde{w}_{kh})(\tilde{z}_{kh}) \\ =: \; & \eta + \eta_{\mathrm{it}}. \end{aligned}$$

Beside the approximation of the weights by the specified projections, we have neglected the remainder term $\mathcal{R}_{kh}$. It is of third order w.r.t. the error e, thus of higher order. Therewith, we are able to define the error estimator η. It should be remarked that the approximation sign "$\approx$" only occurs here in the derivation of the error estimate. In every other step, only real "$=$" signs occur. Furthermore, no other "higher order arguments" are involved. In [31], the derivation is based on the semi- and the full-discrete problem formulation to split the spatial and the temporal error estimator part. There, the unknown semi-discrete solution has to be approximated by the full-discrete one, which involves a higher order argument. In contrast to this, we use the following lemma to split the spatial and the temporal part of the a posteriori error estimate:

Lemma 6. *The following identities hold:*

$$\begin{aligned} \Pi_{k,2h}^{(1,2)} &= i_k^{(1,2)}\Pi_{2h}^{(0,2)} + \Pi_k^{(1,1)} \\ &= i_h^{(1,2)}\Pi_k^{(1,1)} + \Pi_{2h}^{(0,2)}, \\ \Pi_{2k,2h}^{(2,2)} &= i_k^{(2,2)}\Pi_{2h}^{(1,2)} + \Pi_{2k}^{(2,1)} \\ &= i_h^{(2,2)}\Pi_{2k}^{(2,1)} + \Pi_{2h}^{(1,2)}. \end{aligned}$$

Proof. Let φ_{kh} be an arbitrary function from $\mathcal{V}_{kh}^{(1,1)}$. Since φ_{kh} is a tensor product function in

space and time, we obtain

$$\begin{aligned}\Pi^{(2,2)}_{2k,2h}\varphi_{kh} &= i^{(2,2)}_{kh}\varphi_{kh} - i^{(2,1)}_{k}\varphi_{kh} + i^{(2,1)}_{k}\varphi_{kh} - \varphi_{kh}\\ &= i^{(2,2)}_{k}\left(i^{(1,2)}_{h}\varphi_{kh} - \varphi_{kh}\right) + \Pi^{(2,1)}_{2k}\varphi_{kh}\\ &= i^{(2,2)}_{k}\Pi^{(1,2)}_{2h}\varphi_{kh} + \Pi^{(2,1)}_{2k}\varphi_{kh}.\end{aligned}$$

Furthermore, we have

$$\begin{aligned}\Pi^{(2,2)}_{2k,2h}\varphi_{kh} &= i^{(2,2)}_{kh}\varphi_{kh} - \varphi_{kh}\\ &= i^{(2,2)}_{kh}\varphi_{kh} - i^{(1,2)}_{h}\varphi_{kh} + i^{(1,2)}_{h}\varphi_{kh} - \varphi_{kh}\\ &= i^{(2,2)}_{h}\left(i^{(2,1)}_{k}\varphi_{kh} - \varphi_{kh}\right) + \Pi^{(1,2)}_{2h}\varphi_{kh}\\ &= i^{(2,2)}_{h}\Pi^{(1,1)}_{k}\varphi_{kh} + \Pi^{(1,2)}_{2h}\varphi_{kh}.\end{aligned}$$

The indentities for $\Pi^{(1,2)}_{k,2h}$ are derived analogously. □

Definition 7. Let us now define the spatial error estimator terms

$$\begin{aligned}\eta^n_h &:= \frac{1}{2}\left[\rho\left(\tilde{w}_{kh}\right)\left(\Pi^{(0,2)}_{2h}\tilde{z}_{kh}\right) + \rho^\star\left(\tilde{w}_{kh},\tilde{z}_{kh}\right)\left(\Pi^{(1,2)}_{2h}\tilde{w}_{kh}\right)\right],\\ \eta^i_h &:= \frac{1}{2}\left[\rho\left(\tilde{w}_{kh}\right)\left(i^{(1,2)}_{k}\Pi^{(0,2)}_{2h}\tilde{z}_{kh}\right) + \rho^\star\left(\tilde{w}_{kh},\tilde{z}_{kh}\right)\left(i^{(2,2)}_{k}\Pi^{(1,2)}_{2h}\tilde{w}_{kh}\right)\right],\end{aligned}$$

and the temporal error estimator terms

$$\begin{aligned}\eta^n_k &:= \frac{1}{2}\left[\rho\left(\tilde{w}_{kh}\right)\left(\Pi^{(1,1)}_{k}\tilde{z}_{kh}\right) + \rho^\star\left(\tilde{w}_{kh},\tilde{z}_{kh}\right)\left(\Pi^{(2,1)}_{2k}\tilde{w}_{kh}\right)\right],\\ \eta^i_k &:= \frac{1}{2}\left[\rho\left(\tilde{w}_{kh}\right)\left(i^{(1,2)}_{h}\Pi^{(1,1)}_{k}\tilde{z}_{kh}\right) + \rho^\star\left(\tilde{w}_{kh},\tilde{z}_{kh}\right)\left(i^{(2,2)}_{h}\Pi^{(2,1)}_{2k}\tilde{w}_{kh}\right)\right].\end{aligned}$$

Furthermore, we set

$$\begin{aligned}\eta_{ni} &:= \eta^n_h + \eta^i_k,\\ \eta_{in} &:= \eta^i_h + \eta^n_k.\end{aligned}$$

Lemma 6 directly implies the following Corollary:

Corollary 8. *It holds*

$$\eta = \eta_{ni} = \eta_{in}.$$

Here, we focus on η_{ni} as the experiences in [26, Section 1.4] show no differences between the approaches. The numerical results substantiate that both η^n_h and η^i_h measure the spatial error and that η^n_k as well as η^i_k represent the temporal error.

4.4 Localization of the error estimate

The localization in temporal direction is conducted as follows: We split the integral over I into the sum over all subintervals I_m, $0 < m \leq M$ and the error estimate in the initial values. For this purpose, we define

$$\eta^n_h = \sum_{m=0}^{M}\eta^{n,m}_h,\ \eta^i_k = \sum_{m=1}^{M}\eta^{i,m}_k,\ \text{and}\ \eta_{\text{it}} = \sum_{m=1}^{M}\eta^{m}_{\text{it}}.$$

The detailed form of $\eta_k^{i,m}$ is presented in Section C.1 and of $\eta_h^{n,m}$ in Section C.2 in the appendix.

Up to now, we have localized the error estimate to single temporal subintervals. This localization is sufficient for the adaptive temporal refinement. We have to localize the spatial error estimator $\eta_h^{n,m}$ to the single mesh cells in every time step for the spatial mesh refinement. In literature, three different techniques to realize the spatial localization of DWR type error estimators are known: We have cellwise integration by parts of the differential operator, which leads to very complex algorithms, see for instance [4], partition of the unity, cf. [30], and nodal filtering. We apply the third approach, which goes back to [11]. Let

$$\left\{\alpha_j^m : \Omega \to \mathbb{R}^{2d+1} \,\middle|\, j = 1, 2, \ldots, \bar{N}^m := \dim\left(V_h^m\right)^{2d+1}\right\}$$

be the nodal Lagrange basis of $\left(V_h^m\right)^{2d+1}$ and

$$\left\{\beta_j^m : \Omega \to \mathbb{R}^{2d+1} \,\middle|\, j = 1, 2, \ldots, \bar{N}^m\right\}$$

the basis of $\left(V_{2h}^{(2),m}\right)^{2d+1}$. Furthermore, $w_j^m \in \mathbb{R}$, $j = 1, 2, \ldots, \bar{N}^m$, are the coefficients of $\tilde{w}_{kh}^m$, i.e.

$$\tilde{w}_{kh}^m = \sum_{j=1}^{\bar{N}^m} w_j^m \alpha_j^m \quad \text{and} \quad i_{2h}^{(2)} \tilde{w}_{kh}^m = \sum_{j=1}^{\bar{N}^m} w_j^m \beta_j^m.$$

We set $\bar{w}^m = \left(w_1^m, \ldots, w_{\bar{N}^m}^m\right)^\top$. In the same way, we define the coefficients z_j^m of $\tilde{z}_{kh}^m$. The value of the error estimator $\eta_h^{n,m}$ can then be expressed by

$$\eta_h^{n,m} = \sum_{j=1}^{\bar{N}^m} \left(\Psi_j^{P,m} z_j^m + \Psi_j^{D,m} w_j^m\right) + \sum_{j=1}^{\bar{N}^{m-1}} \Lambda_j^{D,m} w_j^{m-1},$$

where $\Psi_j^{P,m}$, $\Psi_j^{D,m}$, and $\Lambda_j^{D,m}$ represent the assembling of the error estimator w.r.t. the difference of the d-quadratic basis $\{\beta_j\}$ and the d-linear one $\{\alpha_j\}$. The space

$$V_{2h}^m := \left\{\varphi \in L^2(\Omega) \,\middle|\, \forall \mathcal{T} \in \mathbb{T}_{2h}^m : \varphi_{|\mathcal{T}} \in Q_1(\mathcal{T}; \mathbb{R})\right\}$$

consists of bilinear basis functions on patches. Because of the patch structure of the meshes, we have $V_{2h}^m \subseteq V_h^m$. The operator $i_{2h}^{(1)} : V_h^m \to V_{2h}^m$ interpolates a function from V_h^m in V_{2h}^m. We define the operator $\pi := \mathrm{id} - i_{2h}^{(1)}$ and call π filtering operator. The nodal vector $\bar{w}^{\pi,m}$ denotes the coefficients of the filtered function $\pi \bar{w}_{kh}^m$ w.r.t. the basis α_j, i.e.

$$\pi \bar{w}_{kh}^m = \sum_{j=1}^{\bar{N}^m} \bar{w}_j^{\pi,m} \alpha_j.$$

The interpolation operator $i_{2h}^{(2)}$ is the identity on V_{2h}^m. Thus, we obtain

$$i_{2h}^{(2)} \pi \alpha_j - \pi \alpha_j = i_{2h}^{(2)} \alpha_j - \alpha_j = \beta_j - \alpha_j.$$

The linearity of the second argument leads to

$$\eta_h^{n,m} = \sum_{j=1}^{\bar{N}^m} \left(\Psi_j^{P,m} z_j^{\pi,m} + \Psi_j^{D,m} w_j^{\pi,m}\right) + \sum_{j=1}^{\bar{N}^{m-1}} \Lambda_j^{D,m} w_j^{\pi,m-1},$$

see [11] for the detailed calculation. We end up with the nodal values $\Psi_j^{P,m} z_j^{\pi,m}$, $\Psi_j^{D,m} w_j^{\pi,m}$, and $\Lambda_j^{D,m} w_j^{\pi,m-1}$, which provide a sufficient localisation, cf. [11]. Finally, the nodal values have to be shifted from the nodes to the cells. We use the method presented in [11], i. e. we simply take the mean value of the values of all nodes, which are the vertices of the mesh cell.

5 Adaptive algorithm

We work with two different approaches to the spatial adaptivity. In the first approach, we set $V_h^m = V_h$ for all $m = 0, 1, \ldots, M$, i. e. the meshes do not change from time step to time step. However, the underlying mesh $\mathbb{T}_h$ is adaptively refined. This method is called constant mesh approach (CM). The alternative is that the meshes can change from time step to time step. We call this the dynamic mesh approach (DM). Using the presented localization methods, we obtain error indicators $\eta_{\mathcal{T}}^{n,m}$ for all $\mathcal{T} \in \mathbb{T}_h^m$ and all $m = 0, 1, \ldots, M$. The sets

$$\begin{aligned}
\Theta_k &:= \left\{ \left|\eta_k^{i,m}\right| \,\middle|\, m = 1, 2, \ldots, M \right\} \\
\Theta_h^{CM} &:= \left\{ \eta_{\mathcal{T}}^n := \sum_{m=0}^{M} \left|\eta_{\mathcal{T}}^{n,m}\right| \,\middle|\, \mathcal{T} \in \mathbb{T}_h \right\}, \\
\Theta_h^{DM} &:= \left\{ \frac{\hat{k}}{k_m} \left|\eta_{\mathcal{T}}^{n,m}\right| \,\middle|\, \mathcal{T} \in \mathbb{T}_h^m,\, m = 0, 1, \ldots, M \right\}
\end{aligned}$$

are the basis for the adaptive refinement, where the scaling factor $\hat{k}/k_m$ with $\hat{k} := T/M$ compensates the linear dependence on k_m of $\eta_{\mathcal{T}}^{n,m}$ in order to obtain globally comparable indicators. In some cases, additional modifications of the spatial indicators may become necessary, cf. [26, Section 2.1]. The numerical error due to the staggered solution scheme is measure by $\eta^N := A\left(\tilde{w}_{kh}\right)\left(\tilde{z}_{kh}\right)$.

The adaptive solution algorithm for the dynamic mesh approach is outlined in detail in Algorithm 11 in Section D and illustrated in Figure 3. We ommit the detials for the constant mesh approach, since it involves only obvious simplifications of the presented algorithm. Let us comment here on the essential parts of the algorithm, where l denotes the current iteration number. We have to specify in advance an initial spatial and temporal mesh as well as the parameters of the staggered solution scheme. Furthermore, a safety factor $c_f \in (0, 1)$, which ensures that the numerical error is some orders smaller than the discretization error, and a equilibration constant $c_e > 1$ for the weighting of spatial and temporal error have to be given. We usually work with $c_f = 10^{-3}$ and $c_e = 5$. The first step is the determination of the solution w_{kh}^l of the primal problem (3). For this purpose, we use the time stepping scheme outlined in Algorithm 9 in Section A in the appendix. Since we need w_{kh} during the solution of the dual problem and the evaluation of the error estimator, we have to save it on the harddisc. These operations are referred to as "primal" in Figure 3. The backward or dual problem (8) is solved in the next step ("dual" in Figure 3), where we use the time stepping scheme outlined in Algorithm 10 in the appendix in Section B. The dual solution z_{kh}^l is also saved on the harddisc, because we need it in the evaluation of the error estimate. The evaluation of the error estimate and the calculation of the refinement indicators is performed next ("estimate" in Figure 3). On one hand, we evaluate the error estimate specified in Definition 7. For this purpose, we evaluate the terms given in Section C.1, C.2, and C.3. On the other hand, we calculate the refinement indicators on each cell, i. e. we have to evaluate the localized form of the error estimator. The refinement indicators are saved on the harddisc for their use in the refinement strategies. After the evaluation of the error estimate,

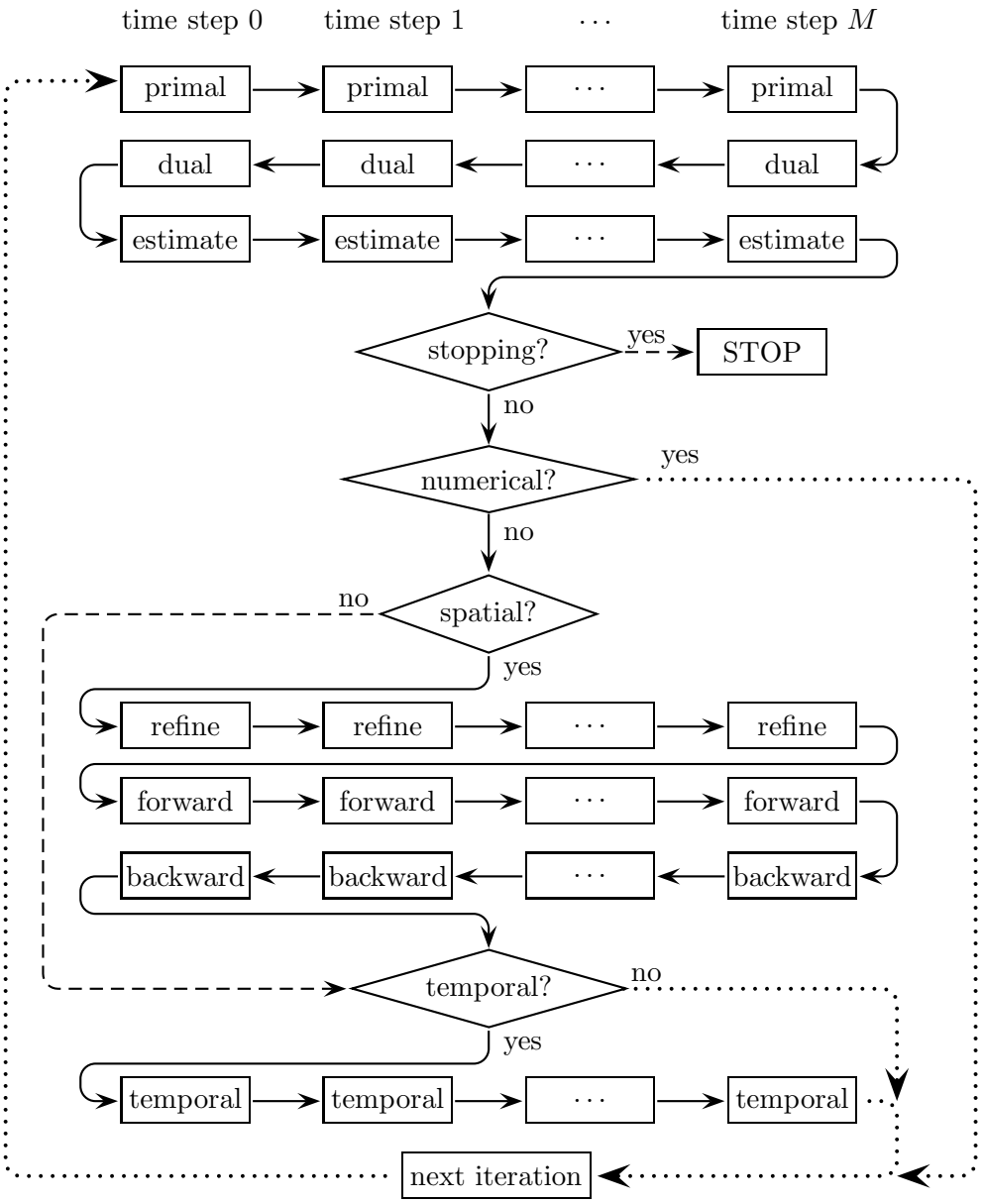

Fig. 3: Illustration of the adaptive solution algorithm based on the dynamic mesh approach

we check the stopping criterion ("stopping?" in Figure 3), for instance if the estimated error is smaller than a given tolerance. If it is fulfilled, we stop the iteration with the desired solution $w_{kh}^{\star}$. If it is not, we test whether the estimated numerical error is small enough, $\left|\eta^{N,l}\right| < c_f \left|\eta^{l}\right|$, or not. When the numerical error is dominant, we directly start a new iteration of the adaptive solution algorithm. Otherwise, we reduce the discretization error by adaptive refinement. The first step of the adaptive refinement procedure is to decide, whether the temporal mesh $\mathbb{T}_k^l$, if

$$\left|\eta_k^{i,l}\right| > c_e \left|\eta_h^{n,l}\right|,$$

the spatial mesh sequence $\mathbb{M}_h^l$, if

$$\left|\eta_h^{n,l}\right| > c_e \left|\eta_k^{i,l}\right|,$$

or both, if

$$c_e \left|\eta_h^{n,l}\right| \geq \left|\eta_k^{i,l}\right| \geq c_e^{-1} \left|\eta_h^{n,l}\right|,$$

should be refined. In Figure 3, we illustrate this step by "spatial?" and "temporal?". A similar strategy can be found in [31]. If no spatial refinement is needed, we set $\mathbb{M}_h^l = \tilde{\mathbb{M}}_h^{l+1}$ and skip the spatial refinement. We begin the spatial refinement with the determination of the set $\Theta_{h,r}^{DM,l}$. It contains all mesh cells, which are chosen for refinement by the optimal mesh strategy, cf. [29]. For the determination of $\Theta_{h,r}^{DM,l}$, all refinement indicators of the mesh sequence $\mathbb{M}_h^l$ are compared. This should lead to a maximum efficient discretisation, since all available information is used in the refinement strategy and it is not restricted to a single time step. For the spatial adaptive refinement, we use the algorithms presented in [26, Chapter 2]. We conduct three single steps here. In the first one, all marked cells are refined. Then, the spatial meshes in each time step are regularized such that they have patch structure and contain only single hanging nodes in space. These two steps are named "refine" in Figure 3. In the last step, mutiple hanging nodes in time are removed. To this end, we need a forward ("forward" in Figure 3) and a backward regularisation ("backward" in Figure 3), cf. [26, Section 2.3]. If it has been decided not to refine the temporal mesh, we set $\mathbb{M}_h^{l+1} = \tilde{\mathbb{M}}_h^l$, $\mathbb{T}_k^{l+1} = \mathbb{T}_k^l$ and skip the temporal refinement. Otherwise, we use again the optimal mesh strategy to determine the set $\Theta_{k,r}^l$. It contains the temporal mesh cells, which are marked for refinement. Then the temporal mesh is adaptively refined. Thereby, we have to modify the spatial mesh sequence $\tilde{\mathbb{M}}_h^{l+1}$, since the number of time steps is changed and a specific spatial mesh is connected to each time step. If a time step is refined, we have to add a spatial mesh, call it $\mathbb{T}_h^{l+1,m+1/2}$, in $\tilde{\mathbb{M}}_h^{l+1}$. Possible choices for $\mathbb{T}_h^{l+1,m+1/2}$ are $\mathbb{T}_h^{l+1,m}$, $\mathbb{T}_h^{l+1,m+1}$ or, e. g., the mesh consisting of the finest cells of $\mathbb{T}_h^{l+1,m}$ and $\mathbb{T}_h^{l+1,m+1}$. We simply insert $\mathbb{T}_h^{l+1,m+1}$. This is referred to as "temporal" in Figure 3. After the adaptive refinement, we increase the number of the iteration cycle l and restart the iteration with the solution of the primal problem.

6 Numerical examples

In this section, we consider several numerical examples concerning the application of our adaptive framework, where two different underlying models are used. The first one consists of linear thermoelasticity, whereas in the second one several nonlinearities are included.

6.1 Linear thermoelasticity

Here, we only shortly present the model of linear thermoelasticity, a more detailed discussion is for instance included in [13]. We set

$$\begin{aligned}
b_1(\varphi,\omega) &:= (\rho\varphi,\omega), \quad \varphi,\omega \in \mathcal{L}^2(\Omega),\\
a_1(u;\theta)(\chi) &:= (\mathbb{C}\varepsilon(u) + \varrho\theta\mathrm{Id}, \varepsilon(\chi)), \quad u,\chi \in \mathcal{H}^1_D(\Omega),\, \theta \in H^1_D(\Omega),\\
l_1(\chi) &:= (f,\chi), \quad \chi \in \mathcal{L}^2(\Omega),\\
b_2(\varphi,\omega) &:= (c_p\rho\varphi,\omega), \quad \varphi,\omega \in L^2(\Omega),\\
a_2(u;\theta)(\chi) &:= (\kappa\nabla\theta,\nabla\chi) + (\varrho\theta_s \mathrm{tr}(\varepsilon(\dot{u})),\chi), \quad u \in \mathcal{H}^1_D(\Omega),\, \theta,\chi \in H^1(\Omega),\\
l_2(\chi) &:= (q,\chi), \quad \chi \in L^2(\Omega).
\end{aligned}$$

Here, the material density is denoted by $\rho > 0$, the linearized strain tensor by $\varepsilon(u) = \frac{1}{2}\left(\nabla u + \nabla u^\top\right)$ as well as the elasticity tensor by $\mathbb{C}$, which is a fourth order tensor determined by the elastic modulus $E > 0$ and Poisson's ratio $\nu \in [0, 0.5)$. The connection between heat and displacement is usually described by the coefficient of thermal expansion $\alpha > 0$. Here, we use the stress-temperature modulus

$$\varrho = -\frac{\alpha E}{1+\nu}\left(\frac{3\nu}{1-2\nu} + 1\right),$$

which leads to a more convenient formulation. The volume forces are given by $f \in L^2\left(I;\mathcal{L}^2(\Omega)\right)$. The specific heat is denoted by $c_p > 0$ and the conductivity by $\kappa > 0$. The heat generated by the elastic deformation is determined by $\varrho\theta_s \mathrm{tr}(\varepsilon(\dot{u}))$. The inner heat source is specified by $q \in L^2\left(I;L^2(\Omega)\right)$.

We choose the domain $\Omega = (0,1)^2$ and homogeneous Dirichlet boundary conditions on $\partial\Omega$, i.e. $\Gamma_D = \partial\Omega$. The time interval is given by $I = [0,1]$. Furthermore, we specify the parameters $\rho = E = \kappa = c_p = 1$, $\nu = 0.3$, and $\alpha = 10^{-3}$ as well as the analytical solution

$$\begin{aligned}
u(x,y,t) &:= \begin{pmatrix} 50\left(t-\frac{1}{3}\right)^{3/2} z(x,y)\left((x-0.5)^2 + (y-0.625)^2\right)^{7/10} \\ 20\left(t-\frac{1}{6}\right)^{3/2} z(x,y)\left(\left(x-0.5-0.0625\sqrt{3}\right)^2 + (y-0.4375)^2\right)^{7/10} \end{pmatrix},\\
\theta(x,y,t) &:= 100\left(t-\frac{2}{3}\right)^{3/2} z(x,y)\left(\left(x-0.5+0.0625\sqrt{3}\right)^2 + (y-0.4375)^2\right)^{7/10},
\end{aligned}$$

with $z(x,y) = x(x-1)\,y(y-1)$. The volume forces f, the inner heat source q, as well as the initial conditions u_s, v_s, and θ_s are calculated based on u and θ. We consider the quantity of interest

$$J(w) = \int_I \int_B u_1 + u_2 + \theta \, dx\, dt = 0.0163187678\ldots$$

with $B = [0.25, 0.75]^2$.

We denote by N the total number of spatial mesh cells and by M the number of time steps. In Table 1, we outline the error estimator η_k^i for a fixed temporal mesh and the estimator η_h^n for a fixed spatial mesh, respectively. We observe that the error estimators are approximately constant, if we vary the spatial mesh for η_k^i and the temporal mesh for η_h^n, respectively. Thus, the estimators η_k^i and η_h^n meet the expectation to be approximately independent of h and k, respectively. A direct consequence of this fact is that the indicators η_h^m depend linearly on k, which needs to be compensated in the adaptive strategy.

l	M	N	η_k^i
1	200	$12,800$	$-2.93158 \cdot 10^{-6}$
2	200	$51,200$	$-9.19793 \cdot 10^{-7}$
3	200	$204,800$	$-6.11811 \cdot 10^{-7}$
4	200	$819,200$	$-5.36550 \cdot 10^{-7}$
5	200	$3,276,800$	$-5.16700 \cdot 10^{-7}$
6	200	$13,107,200$	$-5.11873 \cdot 10^{-7}$
7	200	$52,428,800$	$-5.10674 \cdot 10^{-7}$

l	M	N/M	η_h^n
1	10	$1,024$	$-2.80260 \cdot 10^{-5}$
2	20	$1,024$	$-2.52073 \cdot 10^{-5}$
3	40	$1,024$	$-2.52819 \cdot 10^{-5}$
4	80	$1,024$	$-2.54982 \cdot 10^{-5}$
5	160	$1,024$	$-2.55852 \cdot 10^{-5}$
6	320	$1,024$	$-2.56353 \cdot 10^{-5}$
7	640	$1,024$	$-2.56770 \cdot 10^{-5}$

Tab. 1: Developement of the error estimator η_k^i for fixed temporal and η_h^n for fixed spatial mesh, respectively

l	M	N	L	E_{rel}	I_{eff}
1	10	640	21	$-1.52943 \cdot 10^{-3}$	1.35183
2	20	$5,120$	42	$-3.11951 \cdot 10^{-4}$	1.37868
3	40	$40,960$	80	$-1.10382 \cdot 10^{-4}$	2.05974
4	80	$327,680$	160	$-1.97408 \cdot 10^{-5}$	1.53549
5	160	$2,621,440$	320	$-4.62124 \cdot 10^{-6}$	1.70509
6	320	$20,971,520$	640	$-1.76392 \cdot 10^{-6}$	8.41146
7	640	$167,772,160$	$1,280$	$-1.02975 \cdot 10^{-6}$	2.49093

Tab. 2: Devolopment of the error for uniform refinement in the first example

l	M	N	L	E_{rel}	I_{eff}
1	10	640	10	$-1.5294 \cdot 10^{-3}$	1.35106
2	20	$5,120$	20	$-3.11951 \cdot 10^{-4}$	1.37497
3	40	$36,160$	40	$-1.11967 \cdot 10^{-4}$	2.06148
4	80	$275,840$	80	$-2.03484 \cdot 10^{-5}$	1.49947
5	160	$2,080,000$	160	$-4.93344 \cdot 10^{-6}$	1.38472
6	284	$14,635,088$	284	$-2.05623 \cdot 10^{-6}$	2.04664
7	544	$28,366,336$	544	$-1.47233 \cdot 10^{-6}$	2.45806
8	$1,080$	$221,944,320$	$1,080$	$-1.93684 \cdot 10^{-7}$	1.26259

Tab. 3: Development of the error for adaptive refinement using the constant mesh approach in the first example

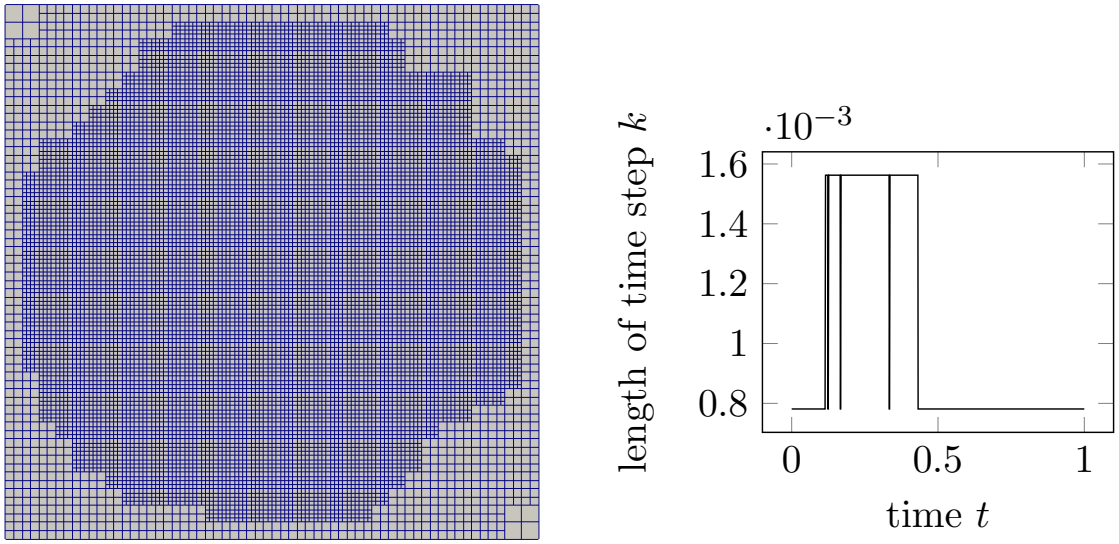

(a) Spatial mesh in the 5^{th} iteration

(b) Temporal mesh in the 8^{th} iteration

Fig. 4: Adaptive meshes in the constant mesh approach

In a second step, we test the adaptive algorithm. Since the spatial singularities of the analytic solution do not depend on time, we work with the constant mesh approach. We denote by L the total number of fixpoint iterations, the relative error by

$$E_{\text{rel}} := \frac{J(w) - J(w_{kh})}{J(w)},$$

and the effectivity index by

$$I_{\text{eff}} := \frac{J(w) - J(w_{kh})}{\eta}.$$

In Table 2, the results for the uniform refinement are listed. We find that the rate of convergence is reduced, which has to be expected because of the low regularity of the analytic solution. The results of the adaptive algorithm using the constant mesh approach are outlined in Table 3. We observe an improved convergence rate and that the estimator is more accurate in the adaptive approach. Exemplary adaptive meshes are depicted in Figure 4. We observe spatial refinements in the midlle of the domain, where the single singularities are not resolved. The temporal mesh is uniformly refined in the majority of the cases. We find smaller time step lengths in the beginning and the end.

6.2 Nonlinear thermoelasticity

In this section, we extend the linear model considered in the last section by some nonlinearities. On the one hand, we assume a linear temperature dependent conductivity, i. e.

$$\kappa(\theta) = \kappa_0 (1 + \beta\theta)$$

with constants $\kappa_0, \beta > 0$. On the other hand, we consider the St. Vernant-Kirchhoff material law taking large deformations into account. Therefore, we define the strain tensor

$$\epsilon(u) = \frac{1}{2}\left(\nabla u + \nabla u^\top + \nabla u^\top \nabla u\right)$$

l	M	N	L	E_{rel}
1	100	19,200	258	$3.55026 \cdot 10^{-2}$
2	200	153,600	516	$6.17390 \cdot 10^{-3}$
3	400	1,228,800	842	$1.16529 \cdot 10^{-3}$
4	800	9,830,400	1,600	$3.59487 \cdot 10^{-4}$
5	1,600	78,643,200	3,200	$9.59380 \cdot 10^{-5}$

Tab. 4: Devolopement of the error for uniform refinement in the second example

and the deformation gradient $F(u) = \mathrm{Id} + \nabla u$. The semilinearform a_1 is then given by

$$a_1(u;\theta)(\chi) := (F(\mathbb{C}\epsilon(u) + \varrho\theta\mathrm{Id}), \varepsilon(\chi)), \quad u, \chi \in \mathcal{H}^1_D(\Omega), \theta \in H^1_D(\Omega).$$

In this example, we consider the L-shaped domain $\Omega = (-0.5, 0.5) \times (-0.5, 0) \cup (-0.5, 0) \times (0, 0.5)$ and the time interval $I = \left[0, 2 + \sqrt{0.125}\right]$. We specify the parameters $\rho = 2700$, $E = 10^6$, $\nu = 0.33$, $\alpha = 24 \cdot 10^{-6}$, $\kappa_0 = 220$, $\beta = 0.05$, and $c_p = 900$. Furthermore, we set the initial conditions and the volume forces to zero. For the displacement and the velocity, we assume homogeneous Dirichlet boundary conditions on $\partial\Omega$, whereas homogeneous Neumann boundary conditions are considered for the temperature on $\partial\Omega$. We define the function

$$c(t) = \begin{cases} (-0.25, 0.5 - t)^\top, & 0 \le t \le t_1, \\ \left(\frac{t-t1}{\sqrt{2}} - 0.25, -\frac{t-t_1}{\sqrt{2}}\right)^\top, & t_1 < t \le t_2, \\ (t - t_2, -0.25)^\top, & t_2 < t \le t_3, \end{cases}$$

with $t_1 = 0.5$, $t_2 = t_1 + \sqrt{0.125}$, and $t_3 = t_2 + 0.5$ as well as the set

$$K(t) = \left\{ (x,y)^\top \in \Omega \,\middle|\, \left| (x,y)^\top - c(t) \right| \le 0.125 \right\},$$

where $|\cdot|$ denotes the Euclidean vector norm. The inner heat source is then given by

$$q(x,y,t) = \begin{cases} 10^8, & t \le t_3 \text{ and } (x,y)^\top \in K(t), \\ 0, & \text{otherwise.} \end{cases}$$

We consider the quantity of interest

$$J(w) = \int_\Omega 10^8 |u(x,y,t_3)|^2 + 10^{-3} (\theta(x,y,t_3))^2 \, dx.$$

Since the analytic solution of the presented example is not known, we calculate a reference value of the quantity of interest by extrapolation over all calculated values of J in the uniform mesh approach and obtain

$$J_{\mathrm{ref}} = 0.10759787968.$$

We use the numerically determined reference value to calculate the relative error. It is outlined for the uniform approach in Table 4 and for the dynamic mesh approach in Table 5. The last value of the adaptive algorithm seems to be more accurate than the reference value such that we ignore the calculated error in this iteration. We achieve with the dynamic mesh approach the approximately same accuracy as with the uniform approach using half the number of unknowns. The temporal mesh is depicted in Figure 5, where large time step lengths are used in the beginning. The adaptive meshes are outlined in Figure 6. We observe only few refinements in the beginning, which follow the heat source. For $t > t_3$, the adptive meshes follow the diffusion of the temperature.

l	M	N	L	E_{rel}
1	100	19,200	100	$3.55049 \cdot 10^{-2}$
2	188	92,700	188	$1.87003 \cdot 10^{-2}$
3	366	633,816	366	$-3.4622 \cdot 10^{-3}$
4	724	4,378,752	724	$-2.5334 \cdot 10^{-4}$
5	1,442	28,424,544	1,442	$-2.8798 \cdot 10^{-4}$

Tab. 5: Development of the error for adaptive refinement using the dynamic mesh approach in the first example

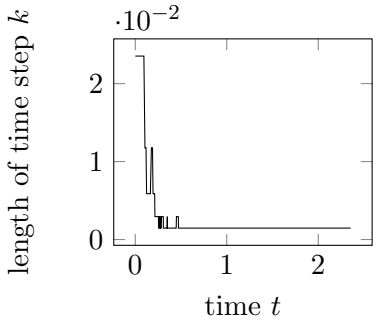

Fig. 5: Temporal mesh in the 5^{th}-iteration of the adaptive algorithm in the second example

7 Conclusions and outlook

In this paper, we present an adaptive algorithm for solving thermomechanical coupled problems, which especially estimates the numerical error introduced by the staggered solution scheme. By this approach, the a posteriori error estimator measures the strength of the coupling between the mechanical and thermal part of the model and can significantly reduce the numerical effort. As usual in DWR methods, we have to introduce some numerical approximation to obtain an evaluable error estimate, which can up to now only be justified by numerical examples, see Section 6, or under high regularity assumptions, cf. [4]. The main disadvantage of the presented approach lies in the fact that we must compute the whole primal and dual solution to obtain an estimate of the numerical error. It would be much better to directly have such an estimate at hand during the solution of the primal problem. It is one topic of further research to construct algorithms, surely involving some additional approximations, which provide such type of information. An other research field is the extension of the presented result to coupled parabolic hyperbolic problems involving plasticity and friction as further sources of heat. However, these problems need a completely different approach because they are modelled by variational inequalities.

Acknowledgement

The author gratefully acknowledges the financial support by the German Research Foundation (DFG) within the subproject A5 of the transregional collaborative research centre (Transregio) 73 “Sheet-Bulk-Metal-Forming”.

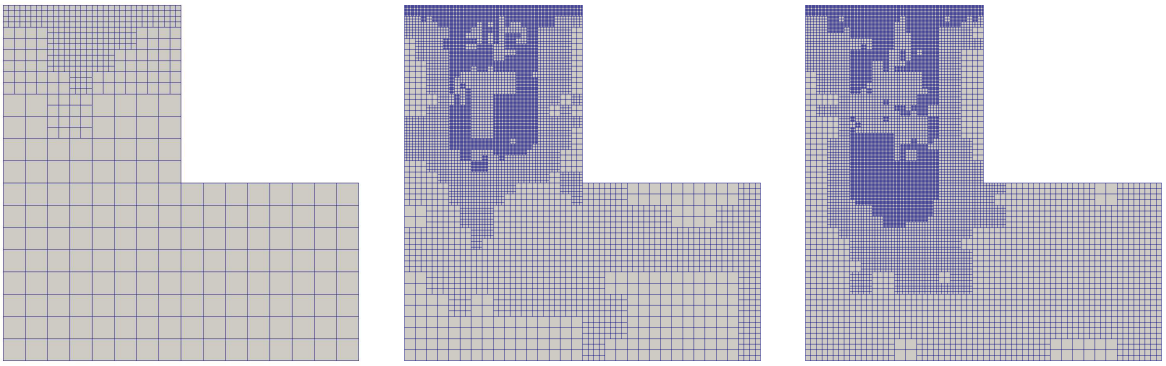

(a) $m = 0$ (b) $m = 100$ (c) $m = 200$

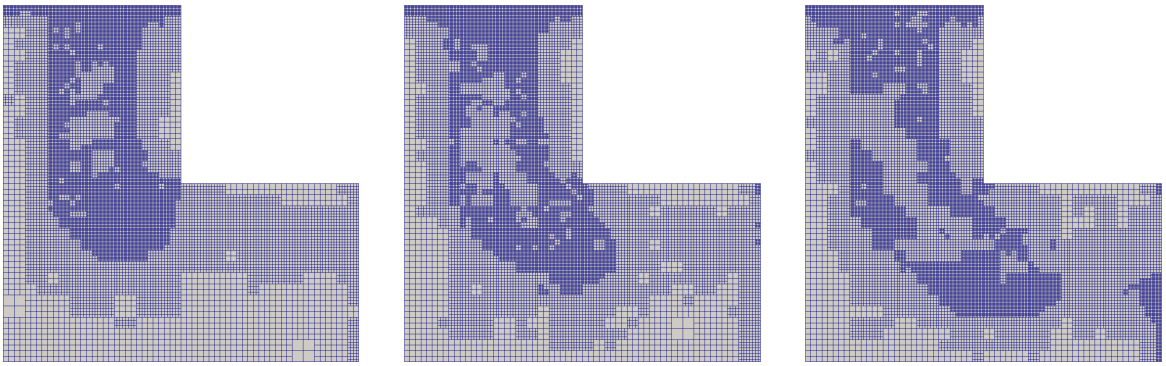

(d) $m = 300$ (e) $m = 400$ (f) $m = 500$

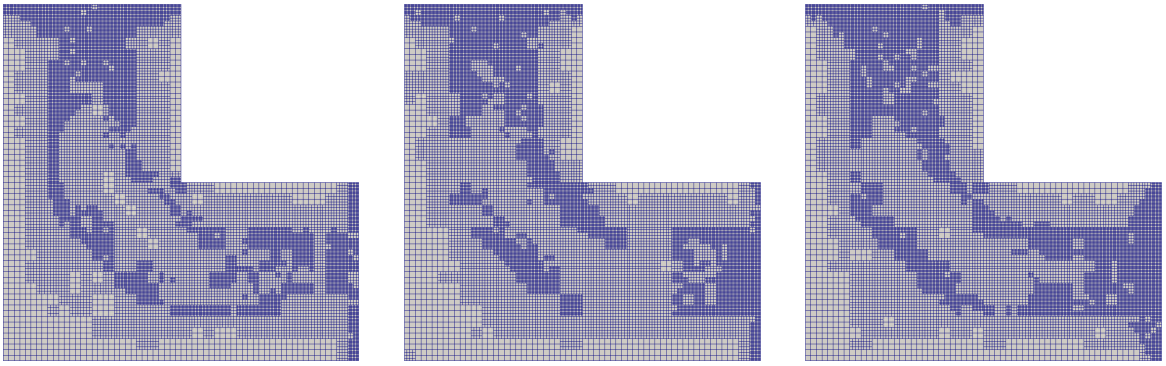

(g) $m = 600$ (h) $m = 700$ (i) $m = 800$

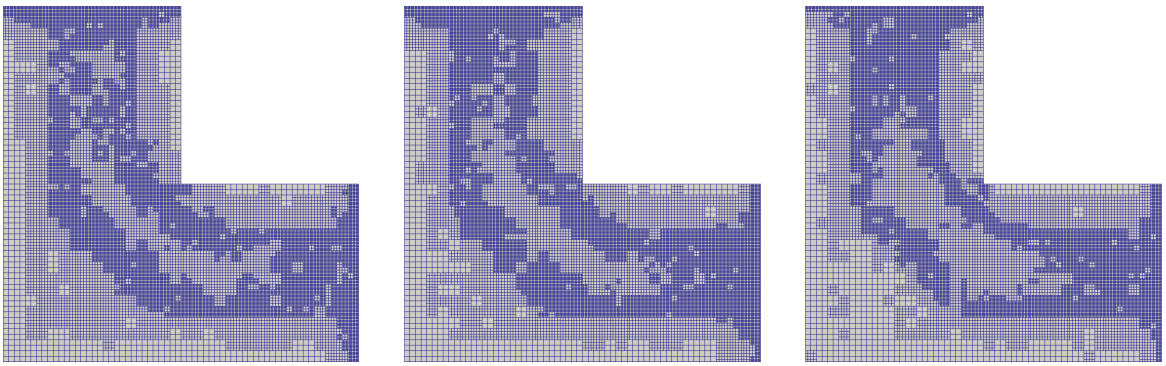

(j) $m = 1000$ (k) $m = 1200$ (l) $m = 1400$

Fig. 6: Adaptive meshes in the 5^{th} iteration of the adaptive algorithm in the second example

References

[1] S. Adjerid. A posteriori finite element error estimation for second-order hyperbolic problems. *Comput. Methods Appl. Mech. Engrg.*, 191:4699–4719, 2002.

[2] D. Aubry, D. Lucas, and B. Tie. Adaptive strategy for transient/coupled problems. Applications to thermoelasticity and elastodynamics. *Comput. Methods Appl. Mech. Engrg.*, 176:41–50, 1999.

[3] W. Bangerth. Adaptive Finite-Elemente-Methoden zur Lösung der Wellengleichung mit Anwendung in der Physik der Sonne. Diploma thesis, Ruprecht-Karls-Universität Heidelberg, 1998.

[4] W. Bangerth and R. Rannacher. *Adaptive Finite Element Methods for Differential Equations.* Birkhäuser, Basel, 2003.

[5] R. Becker. Adaptive finite elements for optimal control problems. Habilitation thesis, Ruprecht-Karls-Universität Heidelberg, 2001.

[6] R. Becker and R. Rannacher. An optimal control approach to a posteriori error estimation and mesh adaptation in finite element methods. In A. Iserles, editor, *Acta Numerica 2000*, pages 1–101. Cambridge University Press, 2001.

[7] C. Bernadi and E. Süli. Time and space adaptivity for the second-order wave equation. *Math. Models Methods Appl. Sci.*, 15(2):199–225, 2005.

[8] D. Biermann, H. Blum, J. Frohne, I. Iovkov, A. Rademacher, and K. Rosin. Simulation of mql deep hole drilling for predicting thermally induced workpiece deformations. *Procedia CIRP*, 2015. accepted.

[9] F. A. Bornemann and M. Schemann. An adaptive Rothe method for the wave equation. *Comput. Visual Sci.*, 1:137–144, 1998.

[10] M. Braack, E. Burman, and N. Taschenberger. Duality based a posteriori error estimation for quasi-periodic solutions using time averages. *SIAM J. Sci. Comput.*, 33(5):2199–2216, 2011.

[11] M. Braack and A. Ern. A posteriori control of modeling errors and discretisation errors. *Multiscale Model. Simul.*, 1(2):221–238, 2003.

[12] M. Braack and N. Taschenberger. A posteriori control of modeling and discretization errors for quasi periodic solutions. *J. Numer. Math.*, 22(2):87–108, 2014.

[13] D. E. Carlson. Linear thermoelasticity. In *Handbuch der Physik*, volume VI a/2, Festkörpermechanik II, pages 297–346. Springer, Berlin, 1972.

[14] K. Eriksson, D. Estep, P. Hansbo, and C. Johnson. *Computational Differential Equations.* Cambridge University Press, Cambridge, 1996.

[15] C. Johnson. Discontinuous Galerkin finite element methods for second order hyperbolic problems. *Comput. Meth. Appl. Mech. Engrg.*, 107:117–129, 1993.

[16] S. Kizio. *Adaptive Finite-Elemente-Algorithmen in der Strukturdynamik*. PhD thesis, Universität Fridericiana zu Karlsruhe, 2008.

[17] S. Kizio and K. Schweizerhof. Time integration error estimation for continuous galerkin schemes. *PAMM, Proc. Appl. Math. Mech.*, 5:675–676, 2005.

[18] A. Kröner. Adaptive finite element methods for optimal control of second order hyperbolic equations. *Comput. Methods Appl. Math.*, 11(2):214 – 240, 2011.

[19] X. Li and N. E. Wiberg. Implementation and adaptivity of a space-time finite element method for structural dynamics. *Comput. Meth. Appl. Mech. Engrg.*, 156:211–229, 1998.

[20] X. Li, N. E. Wiberg, and L. F. Zeng. A posteriori local error estimation and adaptive time-stepping for Newmark integration in dynamic analysis. *Earth. Engng. Struct. Dyn.*, 21:555–571, 1992.

[21] A. Maute. *Fehlerkontrolle bei Finite-Element-Methoden in der linearen Strukturdynamik*. PhD thesis, Universität Stuttgart, 2001.

[22] D. Meidner. *Adaptive Space-Time Finite Element Methods for Optimization Problems Governed by Nonlinear Parabolic Systems*. PhD thesis, Ruprecht-Karls-Universität Heidelberg, 2008.

[23] D. Meidner, R. Rannacher, and J. Vihharev. Goal-oriented error control of the iterative solution of finite element equations. *J. Numer. Math.*, 17(2):143–172, 2009.

[24] D. Meidner and B. Vexler. Adaptive space-time finite element methods for parabolic optimization problems. *SIAM J. Con. Optim.*, 46(1):116–142, 2007.

[25] J. Neumann. *Anwendung von adaptiven Finite Element Algorithmen auf Probleme der Strukturdynamik*. PhD thesis, Universität Fridericiana zu Karlsruhe, 2004.

[26] A. Rademacher. *Adaptive Finite Element Methods for Nonlinear Hyperbolic Problems of Second Order*. PhD thesis, Technische Universität Dortmund, 2009.

[27] R. Rannacher and J. Vihharev. Adaptive finite element analysis of nonlinear problems: balancing of discretization and iteration errors. *J. Numer. Math.*, 21(1):23–61, 2013.

[28] R. Rannacher, A. Westenberger, and W. Wollner. Adaptive finite element solution of eigenvalue problems: Balancing of discretization and iteration error. *J. Numer. Math*, 18(4):303–327, 2010.

[29] T. Richter. *Parallel Multigrid Method for Adaptive Finite Elements with Application to 3D Flow Problems*. PhD thesis, Ruprecht-Karls-Universität Heidelberg, 2005.

[30] T. Richter and T. Wick. Variational localizations of the dual weighted residual estimator. *J. Comput. Appl. Math.*, 279:192–208, 2015.

[31] M. Schmich and B. Vexler. Adaptivity with dynamic meshes for space-time finite element discretizations of parabolic equations. *SIAM J. Sci. Comput.*, 30:369–393, 2008.

[32] G. Simsek, X. Wu, K. G. van der Zee, and E. H. van Brummelen. Duality-based two-level error estimation for time-dependent pdes: Application to linear and nonlinear parabolic equations. *Comput. Methods Appl. Mech. Engrg.*, 2015. in Press.

[33] P. Solin, J. Cerveny, L. Dubcova, and D. Andrs. Monolithic discretization of linear thermoelasticity problems via adaptive multimesh *hp*-FEM. *J. Comput. Appl. Math.*, 234:2350–2357, 2010.

[34] F. Verdugo, N. Parés, and P. Díez. Goal-oriented space-time adaptivity for transient dynamics using a modal description of the adjoint solution. *Comput. Mech.*, 54(2):331–352, 2014.

[35] R. Verfürth. *A Posteriori Error Estimation Techniques for Finite Element Methods*. Oxford University Press, Oxford, 2013.

[36] Y. M. Xie and O. C. Zienkiewicz. A simple error estimator and adaptive time stepping procedure for dynamic analysis. *Earth. Engrg. Struct. Dyn.*, 20:871–887, 1991.

A Primal time stepping scheme

Algorithm 9. Specify a stopping tolerance $\mathrm{TOL} > 0$ and a maximum number of inner iterations $\mathrm{MAX} \in \mathbb{N}$.

1. Calculate the discrete initial values by solving

$$\begin{aligned} \forall \psi_h \in \left(V_h^0\right)^d : \qquad \left(\tilde{u}_{kh}^0, \psi_h\right) &= \left(u_s, \psi_h\right), \\ \forall \chi_h \in \left(V_h^0\right)^d : \qquad \left(\tilde{v}_{kh}^0, \chi_h\right) &= \left(v_s, \chi_h\right), \\ \forall \omega_h \in V_h^0 : \qquad \left(\tilde{\theta}_{kh}^0, \omega_h\right) &= \left(\theta_s, \omega_h\right). \end{aligned}$$

2. Set $m = 1$.

3. Set $l = 1$, $\tilde{u}_{kh}^{m,0} = \mathbb{P}_h^m \tilde{u}_{kh}^{m-1}$, $\tilde{\theta}_{kh}^{m,0} = \mathbb{P}_h^m \tilde{\theta}_{kh}^{m-1}$.

4. Solve the nonlinear equation

$$\begin{aligned} & b_2\left(\tilde{\theta}_{kh}^{m,l}, \omega_h\right) + \frac{1}{2} k_m a_2\left(\tilde{\theta}_{kh}^{m,l}; \tilde{u}_{kh}^{m,l-1}; \tilde{u}_{kh}^{m,l-1}\right)(\omega_h) \\ =& b_2\left(\tilde{\theta}_{kh}^{m-1}, \omega_h\right) - \frac{1}{2} k_m a_2\left(\tilde{\theta}_{kh}^{m-1}; \tilde{u}_{kh}^{m-1}; \tilde{u}_{kh}^{m-1}\right)(\omega_h) + \frac{1}{2} k_m \left[l_2^m(\omega_h) + l_2^{m-1}(\omega_h)\right], \end{aligned} \tag{13}$$

   which has to hold for all $\omega_h \in V_h^m$, w. r. t. $\tilde{\theta}_{kh}^{m,l} \in V_h^m$ by a damped Newton method.

5. Determine the solution $\tilde{u}_{kh}^{m,l} \in (V_h^m)^d$ of the nonlinear equation

$$\begin{aligned} & b_1\left(\tilde{u}_{kh}^{m,l}, \chi_h\right) + \frac{1}{4} k_m^2 a_1\left(\tilde{u}_{kh}^{m,l}; \tilde{\theta}_{kh}^{m,l}\right)(\chi_h) \\ =& b_1\left(\tilde{u}_{kh}^{m-1}, \chi_h\right) + k_m b_1\left(\tilde{v}_{kh}^{m-1}, \chi_h\right) - \frac{1}{4} k_m^2 a_1\left(\tilde{u}_{kh}^{m-1}; \tilde{\theta}_{kh}^{m-1}\right)(\chi_h) \\ & + \frac{1}{4} k_m^2 \left[l_1^m(\chi_h) + l_1^{m-1}(\chi_h)\right] \end{aligned} \tag{14}$$

   for all $\chi_h \in (V_h^m)^d$ using a damped Newton scheme.

6. If $\left\|\tilde{u}_{kh}^{m,l}-\tilde{u}_{kh}^{m,l-1}\right\|+\left\|\tilde{\theta}_{kh}^{m,l}-\tilde{\theta}_{kh}^{m,l-1}\right\|\leq \mathrm{TOL}$ or $i=\mathrm{MAX}$, then set $\tilde{u}_{kh}^{m}=\tilde{u}_{kh}^{m,l}$ and $\tilde{\theta}_{kh}^{m}=\tilde{\theta}_{kh}^{m,l}$, go to 8.
7. Set $l\leftarrow l+1$ and go to 4.
8. Calculate $\tilde{v}_{kh}^{m}\in\left(V_h^m\right)^d$ by solving the linear equation
$$b_1\left(\tilde{v}_{kh}^{m},\psi_h\right)=b_1\left(\frac{2}{k_m}\tilde{u}_{kh}^{m}-\frac{2}{k_m}\tilde{u}_{kh}^{m-1}-\tilde{v}_{kh}^{m-1},\psi_h\right) \tag{15}$$
for all $\psi_h\in\left(V_h^m\right)^d$ using a CG-method.
9. If $m=M$ then STOP.
10. Set $m\leftarrow m+1$ and go to 3.

B Dual time stepping scheme

Algorithm 10. Specify a stopping tolerance $\mathrm{TOL}>0$ and a maximum number of inner iterations $\mathrm{MAX}\in\mathbb{N}$.

1. Set $l=1$, $m=M-1$, $\tilde{\tilde{u}}_{kh}^{M,0}=0$, $\tilde{\tilde{\theta}}_{kh}^{M,0}=0$.
2. Determine the solution $\tilde{\tilde{u}}_{kh}^{M,l}\in\left(V_h^M\right)^d$ of the Helmholtz equation
$$\begin{aligned}&b_1\left(\delta u_h,\tilde{\tilde{u}}_{kh}^{M,l}\right)+\frac{1}{4}k_M^2a'_{1,u}\left(\tilde{u}_{kh}^{M};\tilde{\theta}_{kh}^{M}\right)\left(\delta u_h,\tilde{\tilde{u}}_{kh}^{M,l}\right)\\ =\;&-\frac{1}{4}k_M^2a'_{2,u}\left(\tilde{\theta}_{kh}^{M};\tilde{u}_{kh}^{M}\right)\left(\delta u_h,\tilde{\tilde{\theta}}_{kh}^{M,l}\right)+\frac{1}{4}k_M^2J'_{1,u}\left(\tilde{w}_{kh}^{M}\right)\left(\delta u_h\right)\\ &+\frac{1}{2}k_MJ'_{2,u}\left(\tilde{w}_{kh}^{M}\right)\left(\delta u_h\right)+\frac{1}{2}k_MJ'_{1,v}\left(\tilde{w}_{kh}^{M}\right)\left(\delta u_h\right)+J'_{2,v}\left(\tilde{w}_{kh}^{M}\right)\left(\delta u_h\right)\end{aligned}$$
for all $\delta u_h\in\left(V_h^M\right)^d$ using a CG-method.
3. Solve the Helmholtz equation
$$\begin{aligned}&b_2\left(\delta\theta_h,\tilde{\tilde{\theta}}_{kh}^{M,l}\right)+\frac{1}{2}k_Ma'_{2,\theta}\left(\tilde{\theta}_{kh}^{M};\tilde{u}_{kh}^{M}\right)\left(\delta\theta_h,\tilde{\tilde{\theta}}_{kh}^{M,l}\right)\\ =\;&-\frac{1}{2}k_Ma'_{1,\theta}\left(\tilde{u}_{kh}^{M};\tilde{\theta}_{kh}^{M}\right)\left(\delta\theta_h,\tilde{\tilde{u}}_{kh}^{M,l-1}\right)+\frac{1}{2}k_MJ'_{1,\theta}\left(\tilde{w}_{kh}^{M}\right)\left(\delta\theta_h\right)+J'_{2,\theta}\left(\tilde{w}_{kh}^{M}\right)\left(\delta\theta_h\right),\end{aligned}$$
which has to hold for all $\delta\theta_h\in V_h^M$, w. r. t. $\tilde{\tilde{\theta}}_{kh}^{M,l}\in V_h^M$ by a CG-scheme.
4. If $\left\|\tilde{\tilde{u}}_{kh}^{M,l}-\tilde{\tilde{u}}_{kh}^{M,l-1}\right\|+\left\|\tilde{\tilde{\theta}}_{kh}^{M,l}-\tilde{\tilde{\theta}}_{kh}^{M,l-1}\right\|\leq \mathrm{TOL}$ or $i=\mathrm{MAX}$, then set $\tilde{\tilde{u}}_{kh}^{M}=\tilde{\tilde{u}}_{kh}^{M,l}$ and $\tilde{\tilde{\theta}}_{kh}^{M}=\tilde{\tilde{\theta}}_{kh}^{M,l}$, go to 6.
5. Set $l\leftarrow l+1$ and go to 2.
6. Calculate $\tilde{\tilde{v}}_{kh}^{M}\in\left(V_h^M\right)^d$ by solving the linear equation
$$b_1\left(\delta v_h,\tilde{\tilde{v}}_{kh}^{M}\right)=\frac{2}{k_M}b_1\left(\delta v_h,\tilde{\tilde{u}}_{kh}^{M}\right)-J'_{1,v}\left(\tilde{w}_{kh}^{M}\right)\left(\delta v_h\right)-\frac{2}{k_M}J'_{2,v}\left(\tilde{w}_{kh}^{M}\right)\left(\delta v_h\right)$$
for all $\delta v_h\in\left(V_h^M\right)^d$ using a CG-method.

7. Set $l = 1$, $\tilde{\tilde{u}}_{kh}^{m,0} = \mathbb{P}_h^m \tilde{\tilde{u}}_{kh}^{m+1}$, $\tilde{\tilde{\theta}}_{kh}^{m,0} = \mathbb{P}_h^m \tilde{\tilde{\theta}}_{kh}^{m+1}$.

8. Determine the solution $\tilde{\tilde{u}}_{kh}^{m,l} \in (V_h^m)^d$ of the Helmholtz equation

$$\begin{aligned} & b_1\left(\tilde{\tilde{u}}_{kh}^{m,l}, \delta u_h\right) + \frac{1}{4}k_m^2 a'_{1,u}\left(\tilde{u}_{kh}^m; \tilde{\theta}_{kh}^m\right)\left(\delta u_h, \tilde{\tilde{u}}_{kh}^{m,l}\right) \\ = \; & b_1\left(\tilde{\tilde{u}}_{kh}^{m+1}, \delta u_h\right) + \frac{1}{2}\left(k_m + k_{m+1}\right) b_1\left(\delta u_h, \tilde{\tilde{v}}_{kh}^{m+1}\right) - \frac{1}{4}k_m k_{m+1} a'_{1,u}\left(\tilde{u}_{kh}^m; \tilde{\theta}_{kh}^m\right)\left(\delta u_h, \tilde{\tilde{u}}_{kh}^{m+1}\right) \\ & -\frac{1}{4}k_m^2 a'_{2,u}\left(\tilde{\theta}_{kh}^m; \tilde{u}_{kh}^m\right)\left(\delta u_h, \tilde{\tilde{\theta}}_{kh}^{m,l}\right) - \frac{1}{4}k_m k_{m+1} a'_{2,u}\left(\tilde{\theta}_{kh}^m; \tilde{u}_{kh}^m\right)\left(\delta u_h, \tilde{\tilde{\theta}}_{kh}^{m+1}\right) \\ & +\frac{1}{4}k_m\left(k_m + k_{m+1}\right) J'_{1,u}\left(\tilde{w}_{kh}^m\right)\left(\delta u_h\right) + \frac{1}{2}\left(k_m + k_{m+1}\right) J'_{1,v}\left(\tilde{w}_{kh}^m\right)\left(\delta u_h\right) \end{aligned}$$

   for all $\delta u_h \in (V_h^m)^d$ using a CG-method.

9. Solve the Helmholtz equation

$$\begin{aligned} & b_2\left(\tilde{\tilde{\theta}}_{kh}^m, \delta\theta_h\right) + \frac{1}{2}k_m a'_{2,\theta}\left(\tilde{\theta}_{kh}^m; \tilde{u}_{kh}^m\right)\left(\delta\theta_h, \tilde{\tilde{\theta}}_{kh}^m\right) \\ = \; & b_2\left(\tilde{\tilde{\theta}}_{kh}^{m+1}, \delta\theta_h\right) - \frac{1}{2}k_m a'_{1,\theta}\left(\tilde{u}_{kh}^m; \tilde{\theta}_{kh}^m\right)\left(\delta\theta_h, \tilde{\tilde{u}}_{kh}^m\right) - \frac{1}{2}k_{m+1} a'_{1,\theta}\left(\tilde{u}_{kh}^m; \tilde{\theta}_{kh}^m\right)\left(\delta\theta_h, \tilde{\tilde{u}}_{kh}^{m+1}\right) \\ & -\frac{1}{2}k_{m+1} a'_{2,\theta}\left(\tilde{\theta}_{kh}^m; \tilde{u}_{kh}^m\right)\left(\delta\theta_h, \tilde{\tilde{\theta}}_{kh}^{m+1}\right) + \frac{1}{2}\left(k_m + k_{m+1}\right) J'_{1,\theta}\left(\tilde{w}_{kh}^m\right)\left(\delta\theta_h\right), \end{aligned}$$

   which has to hold for all $\delta\theta_h \in V_h^m$, w. r. t. $\tilde{\tilde{\theta}}_{kh}^{m,l} \in V_h^m$ by a CG-scheme.

10. If $\left\|\tilde{\tilde{u}}_{kh}^{m,l} - \tilde{\tilde{u}}_{kh}^{m,l-1}\right\| + \left\|\tilde{\tilde{\theta}}_{kh}^{m,l} - \tilde{\tilde{\theta}}_{kh}^{m,l-1}\right\| \leq \mathrm{TOL}$ or $i = \mathrm{MAX}$, then set $\tilde{\tilde{u}}_{kh}^m = \tilde{\tilde{u}}_{kh}^{m,l}$ and $\tilde{\tilde{\theta}}_{kh}^m = \tilde{\tilde{\theta}}_{kh}^{m,l}$, go to 12.

11. Set $l \leftarrow l + 1$ and go to 8.

12. Calculate $\tilde{\tilde{v}}_{kh}^m \in (V_h^m)^d$ by solving the linear equation

$$\begin{aligned} b_1\left(\delta v_h, \tilde{\tilde{v}}_{kh}^m\right) \; = \; & -\frac{k_{m+1}}{k_m} b_1\left(\delta v_h, \tilde{\tilde{v}}_{kh}^{m+1}\right) - \frac{2}{k_m} b_1\left(\tilde{\tilde{u}}_{kh}^{m+1} - \tilde{\tilde{u}}_{kh}^m, \delta v_h\right) \\ & -\left(\frac{k_m + k_{m+1}}{k_m}\right) J'_{1,v}\left(\tilde{w}_{kh}^m\right)\left(\delta v_h\right) \end{aligned}$$

   for all $\delta v_h \in (V_h^m)^d$ using a CG-method.

13. If $m = 1$ then go to 15.

14. Set $m \leftarrow m - 1$ and go to 7.

15. Solve the linear equation

$$\begin{aligned} b_2\left(\tilde{\tilde{\theta}}_{kh}^0, \delta\theta_h\right) \; = \; & -\frac{1}{2}k_1 a'_{1,\theta}\left(\tilde{u}_{kh}^0; \tilde{\theta}_{kh}^0\right)\left(\delta\theta_h, \tilde{\tilde{u}}_{kh}^1\right) - \frac{1}{2}k_1 a'_{2,\theta}\left(\tilde{\theta}_{kh}^0; \tilde{u}_{kh}^0\right)\left(\delta\theta_h, \tilde{\tilde{\theta}}_{kh}^1\right) \\ & +b_2\left(\tilde{\tilde{\theta}}_{kh}^1, \delta\theta_h\right) + \frac{1}{2}k_1 J'_{1,\theta}\left(\tilde{w}_{kh}^0\right)\left(\delta\theta_h\right) \end{aligned}$$

   which has to hold for all $\delta\theta_h \in V_h^0$, w. r. t. $\tilde{\tilde{\theta}}_{kh}^0 \in V_h^0$ by a CG-scheme.

16. Determine the solution $\tilde{\tilde{u}}^0_{kh} \in \left(V_h^0\right)^d$ of the linear equation

$$b_1\left(\tilde{\tilde{u}}^0_{kh}, \delta v_h\right) = \frac{1}{2}k_1 b_1\left(\delta v_h, \tilde{\tilde{v}}^1_{kh}\right) + b_1\left(\tilde{\tilde{u}}^1_{kh}, \delta v_h\right) + \frac{1}{2}k_1 J'_{1,v}\left(\tilde{w}^0_{kh}\right)\left(\delta v_h\right)$$

for all $\delta u_h \in \left(V_h^0\right)^d$ using a CG-method.

17. Calculate $\tilde{\tilde{v}}^0_{kh} \in \left(V_h^0\right)^d$ by solving the linear equation

$$\begin{aligned} b_1\left(\tilde{\tilde{v}}^0_{kh}, \delta u_h\right) &= -\frac{1}{2}k_1 a'_{1,u}\left(\tilde{u}^0_{kh}; \tilde{\theta}^0_{kh}\right)\left(\delta u_h, \tilde{\tilde{u}}^1_{kh}\right) - \frac{1}{2}k_1 a'_{2,u}\left(\tilde{\theta}^0_{kh}; \tilde{u}^0_{kh}\right)\left(\delta u_h, \tilde{\tilde{\theta}}^1_{kh}\right) \\ &\quad + b_1\left(\tilde{\tilde{v}}^1_{kh}, \delta u_h\right) + \frac{1}{2}k_1 J'_{1,u}\left(\tilde{w}^0_{kh}\right)\left(\delta u_h\right) \end{aligned}$$

for all $\delta v_h \in \left(V_h^0\right)^d$ using a CG-method.

C Concrete terms of the error estimator

Here, we collect the concrete terms of the error estimator w.r.t. the temporal and the spatial part.

C.1 Temporal error estimate

This section is devoted to the detailed derivation of the temporal error estimator. For the evaluation of the a posteriori error estimate, two different interpolation methods of higher order in time are needed. The first one is $i_k^{(1)}$, which is linear and is used in the case of piecewise constant trial functions. The other one is $i_{2k}^{(2)}$, which is quadratic. Piecewise linear functions are extrapolated by this method. The interpolation operator $i_k^{(1)}$ is defined as

$$i_k^{(1)} v_{kh}(t) := \frac{t_m - t}{k_m} v_{kh}^{m-1} + \frac{t - t_{m-1}}{k_m} v_{kh}^m$$

with $t \in I_m$ and $v_{kh} \in W_{kh}$. The evaluation of the interpolation at different time instances results in the terms

$$\begin{aligned} i_k^{(1)} v_{kh}\left(t_m\right) &= v_{kh}^m \\ i_k^{(1)} v_{kh}\left(t_{m-1}\right) &= v_{kh}^{m-1} \\ i_k^{(1)} v_{kh}\left(t_{m-\frac{1}{2}}\right) &= \frac{1}{2}k_m\left[v_{kh}^m + v_{kh}^{m-1}\right]. \end{aligned}$$

The interpolation operator $i_{2k}^{(2)}$ is defined as

$$\begin{aligned} i_{2k}^{(2)} v_{kh}(t) &:= \frac{\left(t_m - t\right)\left(t_{m+1} - t\right)}{k_m\left(k_m + k_{m+1}\right)} v_{kh}^{m-1} + \frac{\left(t - t_{m-1}\right)\left(t_{m+1} - t\right)}{k_m k_{m+1}} v_{kh}^m \\ &\quad + \frac{\left(t - t_{m-1}\right)\left(t - t_m\right)}{\left(k_m + k_{m+1}\right)k_{m+1}} v_{kh}^{m+1} \end{aligned}$$

for $t \in I_m \cup I_{m+1}$ and $v_{kh} \in V_{kh}$. The basic evaluation terms are

$$i_{2k}^{(2)} v_{kh}\left(t_{m-1}\right) = v_{kh}^{m-1}, \quad i_{2k}^{(2)} v_{kh}\left(t_m\right) = v_{kh}^m, \quad i_{2k}^{(2)} v_{kh}\left(t_{m+1}\right) = v_{kh}^{m+1}$$

and

$$\begin{aligned} i_{2k}^{(2)} v_{kh}\left(t_{m-\frac{1}{2}}\right) &= \frac{1}{2}\frac{k_{m+1}+\frac{1}{2}k_m}{k_m+k_{m+1}} v_{kh}^{m-1} + \frac{1}{2}\left(1+\frac{k_m}{2k_{m+1}}\right) v_{kh}^{m} \\ &\quad -\frac{1}{4}\frac{k_m^2}{(k_m+k_{m+1})\,k_{m+1}} v_{kh}^{m+1} \\ i_{2k}^{(2)} v_{kh}\left(t_{m+\frac{1}{2}}\right) &= -\frac{1}{4}\frac{k_{m+1}^2}{k_m\,(k_m+k_{m+1})} v_{kh}^{m-1} + \frac{1}{2}\left(1+\frac{k_{m+1}}{2k_m}\right) v_{kh}^{m} \\ &\quad +\frac{1}{2}\frac{k_m+\frac{1}{2}k_{m+1}}{k_m+k_{m+1}} v_{kh}^{m+1} \end{aligned}$$

with

$$t_{m-\frac{1}{2}} = \frac{1}{2}\left(t_{m-1}+t_m\right) \quad \text{and} \quad t_{m+\frac{1}{2}} = \frac{1}{2}\left(t_m+t_{m+1}\right).$$

Using this interpolation ansatz, we are able to write down the temporal error estimator

$$\begin{aligned} & \eta_k^{i,m} \\ = \;& \frac{1}{2}\left[\rho\left(\tilde{w}_{kh}\right)\left(i_{2h}^{(2)}\Pi_k^{(1)}\tilde{z}_{kh}\right)_m + \rho^\star\left(\tilde{w}_{kh},\tilde{z}_{kh}\right)\left(i_{2h}^{(2)}\Pi_{2k}^{(2)}\tilde{w}_{kh}\right)_m\right] \\ = \;& \left[-\frac{1}{2}A\left(\tilde{w}_{kh}\right)\left(i_{2h}^{(2)}\Pi_k^{(1)}\tilde{z}_{kh}\right)\right]_m + \left[\frac{1}{2}J_1'\left(\tilde{w}_{kh}\right)\left(i_{2h}^{(2)}\Pi_{2k}^{(2)}\tilde{w}_{kh}\right) - \frac{1}{2}A'\left(\tilde{w}_{kh}\right)\left(i_{2h}^{(2)}\Pi_{2k}^{(2)}\tilde{w}_{kh}\right)\right]_m \\ =: \;& \left[\eta_{k,pu}^m + \eta_{k,pv}^m + \eta_{k,p\theta}^m\right] + \left[\eta_{k,d\bar{u}}^m + \eta_{k,d\bar{v}}^m + \eta_{k,d\bar{\theta}}^m\right] \end{aligned}$$

for $0 < m < M$. Using suitable quadrature rules, we obtain for the single terms

$$\begin{aligned} \eta_{k,pu}^m &= -\frac{1}{2}\left[\left(b_1\left(\dot{\tilde{v}}_{kh}, i_{2h}^{(2)}\Pi_k^{(1)}\tilde{\tilde{u}}_{kh}\right)\right)_m + \left(a_1\left(\tilde{u}_{kh};\tilde{\theta}_{kh}\right)\left(i_{2h}^{(2)}\Pi_k^{(1)}\tilde{\tilde{u}}_{kh}\right)\right)_m\right] \\ &\quad +\frac{1}{2}\left(l_1\left(i_{2h}^{(2)}\Pi_k^{(1)}\tilde{\tilde{u}}_{kh}\right)\right)_m \\ &= \frac{1}{4}b_1\left(\tilde{v}_{kh}^m - \tilde{v}_{kh}^{m-1}, i_{2h}^{(2)}\left(\tilde{\tilde{u}}_{kh}^m - \tilde{\tilde{u}}_{kh}^{m-1}\right)\right) + \frac{k_m}{6}a_1\left(\tilde{u}_{kh}^m;\tilde{\theta}_{kh}^m\right)\left(i_{2h}^{(2)}\tilde{\tilde{u}}_{kh}^m\right) \\ &\quad -\frac{k_m}{6}a_1\left(\tilde{u}_{kh}^{m-\frac{1}{2}};\tilde{\theta}_{kh}^{m-\frac{1}{2}}\right)\left(i_{2h}^{(2)}\left(\tilde{\tilde{u}}_{kh}^m + \tilde{\tilde{u}}_{kh}^{m-1}\right)\right) \\ &\quad -\frac{k_m}{12}a_1\left(\tilde{u}_{kh}^{m-1};\tilde{\theta}_{kh}^{m-1}\right)\left(i_{2h}^{(2)}\left(\tilde{\tilde{u}}_{kh}^{m-1} - 3\tilde{\tilde{u}}_{kh}^m\right)\right) \\ &\quad +\frac{k_m}{12}\left[-2l_1^m\left(i_{2h}^{(2)}\tilde{\tilde{u}}_{kh}^m\right) + 2l_1^{m-\frac{1}{2}}\left(i_{2h}^{(2)}\left(\tilde{\tilde{u}}_{kh}^m + \tilde{\tilde{u}}_{kh}^{m-1}\right)\right) + l_1^{m-1}\left(i_{2h}^{(2)}\left(\tilde{\tilde{u}}_{kh}^{m-1} - 3\tilde{\tilde{u}}_{kh}^m\right)\right)\right], \end{aligned}$$

$$\begin{aligned} \eta_{k,pv}^m &= -\frac{1}{2}\left(b_1\left(\dot{\tilde{u}}_{kh} - \tilde{v}_{kh}, i_{2h}^{(2)}\Pi_k^{(1)}\tilde{\tilde{v}}_{kh}\right)\right)_m \\ &= \frac{1}{4}b_1\left(\tilde{u}_{kh}^m - \tilde{u}_{kh}^{m-1}, i_{2h}^{(2)}\left(\tilde{\tilde{v}}_{kh}^m - \tilde{\tilde{v}}_{kh}^{m-1}\right)\right) - \frac{1}{12}k_m b_1\left(\tilde{v}_{kh}^m + 2\tilde{v}_{kh}^{m-1}, i_{2h}^{(2)}\left(\tilde{\tilde{v}}_{kh}^m - \tilde{\tilde{v}}_{kh}^{m-1}\right)\right), \end{aligned}$$

$$
\begin{aligned}
\eta^m_{k,p\theta} &= -\frac{1}{2}\left[\left(b_2\left(\dot{\tilde{\theta}}_{kh}, i^{(2)}_{2h}\Pi^{(1)}_k\tilde{\bar{\theta}}_{kh}\right)\right)_m + \left(a_2\left(\tilde{\theta}_{kh};\tilde{u}_{kh}\right)\left(i^{(2)}_{2h}\Pi^{(1)}_k\tilde{\bar{\theta}}_{kh}\right)\right)_m\right]\\
&\quad +\frac{1}{2}\left(l_2\left(i^{(2)}_{2h}\Pi^{(1)}_k\tilde{\bar{\theta}}_{kh}\right)\right)_m\\
&= \frac{1}{4}b_2\left(\tilde{\theta}^m_{kh}-\tilde{\theta}^{m-1}_{kh}, i^{(2)}_{2h}\left(\tilde{\bar{\theta}}^m_{kh}-\tilde{\bar{\theta}}^{m-1}_{kh}\right)\right)+\frac{k_m}{6}a_2\left(\tilde{u}^m_{kh};\tilde{\theta}^m_{kh}\right)\left(i^{(2)}_{2h}\tilde{\bar{\theta}}^m_{kh}\right)\\
&\quad -\frac{k_m}{6}a_2\left(\tilde{u}^{m-\frac{1}{2}}_{kh};\tilde{\theta}^{m-\frac{1}{2}}_{kh}\right)\left(i^{(2)}_{2h}\left(\tilde{\bar{\theta}}^m_{kh}+\tilde{\bar{\theta}}^{m-1}_{kh}\right)\right)\\
&\quad -\frac{k_m}{12}a_2\left(\tilde{u}^{m-1}_{kh};\tilde{\theta}^{m-1}_{kh}\right)\left(i^{(2)}_{2h}\left(\tilde{\bar{\theta}}^{m-1}_{kh}-3\tilde{\bar{\theta}}^m_{kh}\right)\right)\\
&\quad +\frac{k_m}{12}\left[-2l^m_2\left(i^{(2)}_{2h}\tilde{\bar{\theta}}^m_{kh}\right)+2l^{m-\frac{1}{2}}_2\left(i^{(2)}_{2h}\left(\tilde{\bar{\theta}}^m_{kh}+\tilde{\bar{\theta}}^{m-1}_{kh}\right)\right)+l^{m-1}_2\left(i^{(2)}_{2h}\left(\tilde{\bar{\theta}}^{m-1}_{kh}-3\tilde{\bar{\theta}}^m_{kh}\right)\right)\right],
\end{aligned}
$$

$$
\begin{aligned}
\eta^m_{k,d\bar{u}} &= \frac{1}{2}\int_{I_m} J'_{1,u}\left(\tilde{w}_{kh}\right)\left(i^{(2)}_{2h}\Pi^{(2)}_{2k}\tilde{u}_{kh}\right)\,dt-\frac{1}{2}\left(a'_{1,u}\left(\tilde{u}_{kh};\tilde{\theta}_{kh}\right)\left(i^{(2)}_{2h}\Pi^{(2)}_{2k}\tilde{u}_{kh},\tilde{\bar{u}}_{kh}\right)\right)_m\\
&\quad -\frac{1}{2}\left(a'_{2,u}\left(\tilde{\theta}_{kh};\tilde{u}_{kh}\right)\left(i^{(2)}_{2h}\Pi^{(2)}_{2k}\tilde{u}_{kh},\tilde{\bar{\theta}}_{kh}\right)\right)_m+\frac{1}{2}b_1\left(\left[\tilde{\bar{v}}_{kh}\right]_m, i^{(2)}_{2h}\Pi^{(2)}_{2k}\tilde{u}^m_{kh}\right)\\
&= -\frac{k_m}{6}\left[J'_{1,u}\left(\tilde{w}^m_{kh}\right)\left(i^{(2)}_{2h}\tilde{u}^m_{kh}\right)+J'_{1,u}\left(\tilde{w}^{m-1}_{kh}\right)\left(i^{(2)}_{2h}\tilde{u}^{m-1}_{kh}\right)\right]\\
&\quad +\frac{k_m}{3}J'_{1,u}\left(\tilde{w}^{m-\frac{1}{2}}_{kh}\right)\left(i^{(2)}_{2h}i^{(2)}_{2k}\tilde{u}^{m-\frac{1}{2}}_{kh}\right)\\
&\quad +\frac{k_m}{6}\left[a'_{1,u}\left(\tilde{u}^m_{kh};\tilde{\theta}^m_{kh}\right)\left(i^{(2)}_{2h}\tilde{u}^m_{kh},\tilde{\bar{u}}^m_{kh}\right)+a'_{1,u}\left(\tilde{u}^{m-1}_{kh};\tilde{\theta}^{m-1}_{kh}\right)\left(i^{(2)}_{2h}\tilde{u}^{m-1}_{kh},\tilde{\bar{u}}^m_{kh}\right)\right]\\
&\quad -\frac{k_m}{3}a'_{1,u}\left(\tilde{u}^{m-\frac{1}{2}}_{kh};\tilde{\theta}^{m-\frac{1}{2}}_{kh}\right)\left(i^{(2)}_{2h}i^{(2)}_{2k}\tilde{u}^{m-\frac{1}{2}}_{kh},\tilde{\bar{u}}^m_{kh}\right)\\
&\quad +\frac{k_m}{6}\left[a'_{2,u}\left(\tilde{\theta}^m_{kh};\tilde{u}^m_{kh}\right)\left(i^{(2)}_{2h}\tilde{u}^m_{kh},\tilde{\bar{\theta}}^m_{kh}\right)+a'_{2,u}\left(\tilde{\theta}^{m-1}_{kh};\tilde{u}^{m-1}_{kh}\right)\left(i^{(2)}_{2h}\tilde{u}^{m-1}_{kh},\tilde{\bar{\theta}}^m_{kh}\right)\right]\\
&\quad -\frac{k_m}{3}a'_{2,u}\left(\tilde{\theta}^{m-\frac{1}{2}}_{kh};\tilde{u}^{m-\frac{1}{2}}_{kh}\right)\left(i^{(2)}_{2h}i^{(2)}_{2k}\tilde{u}^{m-\frac{1}{2}}_{kh},\tilde{\bar{\theta}}^m_{kh}\right),
\end{aligned}
$$

$$
\begin{aligned}
\eta^m_{k,d\bar{v}} &= \frac{1}{2}\int_{I_m} J'_{1,v}\left(\tilde{w}_{kh}\right)\left(i^{(2)}_{2h}\Pi^{(2)}_{2k}\tilde{v}_{kh}\right)\,dt\\
&\quad +\frac{1}{2}\left[\left(b_1\left(i^{(2)}_{2h}\Pi^{(2)}_{2k}\tilde{v}_{kh},\tilde{\bar{v}}_{kh}\right)\right)_m+b_1\left(\left[\tilde{\bar{v}}_{kh}\right]_m, i^{(2)}_{2h}\Pi^{(2)}_{2k}\tilde{v}^m_{kh}\right)\right]\\
&= -\frac{k_m}{6}\left[J'_{1,v}\left(\tilde{w}^m_{kh}\right)\left(i^{(2)}_{2h}\tilde{v}^m_{kh}\right)+J'_{1,v}\left(\tilde{w}^{m-1}_{kh}\right)\left(i^{(2)}_{2h}\tilde{v}^{m-1}_{kh}\right)\right]\\
&\quad +\frac{k_m}{3}J'_{1,v}\left(\tilde{w}^{m-\frac{1}{2}}_{kh}\right)\left(i^{(2)}_{2h}i^{(2)}_{2k}\tilde{v}^{m-\frac{1}{2}}_{kh}\right)\\
&\quad -\frac{k_m}{6}b_1\left(i^{(2)}_{2h}\left(\tilde{v}^m_{kh}+\tilde{v}^{m-1}_{kh}\right),\tilde{\bar{v}}^m_{kh}\right)+\frac{k_m}{3}b_1\left(i^{(2)}_{2h}i^{(2)}_{2k}\tilde{v}^{m-\frac{1}{2}}_{kh},\tilde{\bar{v}}^m_{kh}\right),
\end{aligned}
$$

$$
\begin{aligned}
\eta_{k,d\bar{\theta}}^m &= \frac{1}{2}\int_{I_m} J'_{1,\theta}\left(\tilde{w}_{kh}\right)\left(i_{2h}^{(2)}\Pi_{2k}^{(2)}\tilde{\theta}_{kh}\right)\,dt - \frac{1}{2}\left(a'_{1,\theta}\left(\tilde{u}_{kh};\tilde{\theta}_{kh}\right)\left(i_{2h}^{(2)}\Pi_{2k}^{(2)}\tilde{\theta}_{kh},\tilde{\bar{\theta}}_{kh}\right)\right)_m \\
&\quad -\frac{1}{2}\left(a'_{2,\theta}\left(\tilde{\theta}_{kh};\tilde{u}_{kh}\right)\left(i_{2h}^{(2)}\Pi_{2k}^{(2)}\tilde{\theta}_{kh},\tilde{\bar{\theta}}_{kh}\right)\right)_m + \frac{1}{2}b_2\left(\left[\tilde{\bar{\theta}}_{kh}\right]_m, i_{2h}^{(2)}\Pi_{2k}^{(2)}\tilde{\theta}_{kh}^m\right) \\
&= -\frac{k_m}{6}\left[J'_{1,\theta}\left(\tilde{w}_{kh}^m\right)\left(i_{2h}^{(2)}\tilde{\theta}_{kh}^m\right) + J'_{1,\theta}\left(\tilde{w}_{kh}^{m-1}\right)\left(i_{2h}^{(2)}\tilde{\theta}_{kh}^{m-1}\right)\right] \\
&\quad +\frac{k_m}{3}J'_{1,\theta}\left(\tilde{w}_{kh}^{m-\frac{1}{2}}\right)\left(i_{2h}^{(2)}i_{2k}^{(2)}\tilde{\theta}_{kh}^{m-\frac{1}{2}}\right) \\
&\quad +\frac{k_m}{6}\left[a'_{1,\theta}\left(\tilde{u}_{kh}^m;\tilde{\theta}_{kh}^m\right)\left(i_{2h}^{(2)}\tilde{\theta}_{kh}^m,\tilde{\bar{u}}_{kh}^m\right) + a'_{1,\theta}\left(\tilde{u}_{kh}^{m-1};\tilde{\theta}_{kh}^{m-1}\right)\left(i_{2h}^{(2)}\tilde{\theta}_{kh}^{m-1},\tilde{\bar{u}}_{kh}^m\right)\right] \\
&\quad -\frac{k_m}{3}a'_{1,\theta}\left(\tilde{u}_{kh}^{m-\frac{1}{2}};\tilde{\theta}_{kh}^{m-\frac{1}{2}}\right)\left(i_{2h}^{(2)}i_{2k}^{(2)}\tilde{\theta}_{kh}^{m-\frac{1}{2}},\tilde{\bar{u}}_{kh}^m\right) \\
&\quad +\frac{k_m}{6}\left[a'_{2,\theta}\left(\tilde{\theta}_{kh}^m;\tilde{u}_{kh}^m\right)\left(i_{2h}^{(2)}\tilde{\theta}_{kh}^m,\tilde{\bar{\theta}}_{kh}^m\right) + a'_{2,\theta}\left(\tilde{\theta}_{kh}^{m-1};\tilde{u}_{kh}^{m-1}\right)\left(i_{2h}^{(2)}\tilde{\theta}_{kh}^{m-1},\tilde{\bar{\theta}}_{kh}^m\right)\right] \\
&\quad -\frac{k_m}{3}a'_{2,\theta}\left(\tilde{u}_{kh}^{m-\frac{1}{2}};\tilde{\theta}_{kh}^{m-\frac{1}{2}}\right)\left(i_{2h}^{(2)}i_{2k}^{(2)}\tilde{\theta}_{kh}^{m-\frac{1}{2}},\tilde{\bar{\theta}}_{kh}^m\right).
\end{aligned}
$$

C.2 Spatial error estimate

In this section, we give the single terms of the spatial error estimator η_h^n. In the first time step, we obtain

$$
\begin{aligned}
\eta_h^{n,0} &= -\frac{1}{2}\left[b_1\left(\tilde{u}_{kh}^0 - u_s, \Pi_{2h}^{(2)}\tilde{\bar{v}}_{kh}^0\right) + b_1\left(\tilde{v}_{kh}^0 - v_s, \Pi_{2h}^{(2)}\tilde{\bar{u}}_{kh}^0\right) + b_2\left(\tilde{\theta}_{kh}^0 - \theta_s, \Pi_{2h}^{(2)}\tilde{\bar{\theta}}_{kh}^0\right)\right] \\
&\quad +\frac{1}{2}\left[b_1\left(\tilde{\bar{u}}_{kh}^1 - \tilde{\bar{u}}_{kh}^0, \Pi_{2h}^{(2)}\tilde{v}_{kh}^0\right) + b_1\left(\tilde{\bar{v}}_{kh}^1 - \tilde{\bar{v}}_{kh}^0, \Pi_{2h}^{(2)}\tilde{u}_{kh}^0\right) + b_2\left(\tilde{\bar{\theta}}_{kh}^1 - \tilde{\bar{\theta}}_{kh}^0, \Pi_{2h}^{(2)}\tilde{\theta}_{kh}^0\right)\right]
\end{aligned}
$$

For a time step $0 < m < M$, it holds

$$
\begin{aligned}
&\eta_h^{n,m} \\
&= \frac{1}{2}\left[\rho\left(\tilde{w}_{kh}\right)\left(\Pi_{2h}^{(0,2)}\tilde{z}_{kh}\right)_m + \rho^\star\left(\tilde{w}_{kh},\tilde{z}_{kh}\right)\left(\Pi_{2h}^{(1,2)}\tilde{w}_{kh}\right)_m\right] \\
&= \left[-\frac{1}{2}A\left(\tilde{w}_{kh}\right)\left(\Pi_{2h}^{(0,2)}\tilde{z}_{kh}\right)\right]_m + \left[\frac{1}{2}J'_1\left(\tilde{w}_{kh}\right)\left(\Pi_{2h}^{(1,2)}\tilde{w}_{kh}\right) - \frac{1}{2}A'\left(\tilde{w}_{kh}\right)\left(\Pi_{2h}^{(1,2)}\tilde{w}_{kh},\tilde{z}_{kh}\right)\right]_m \\
&=: \left[\eta_{h,pu}^m + \eta_{h,pv}^m + \eta_{h,p\theta}^m\right] + \left[\eta_{h,d\bar{u}}^m + \eta_{h,d\bar{v}}^m + \eta_{h,d\bar{\theta}}^m\right].
\end{aligned}
$$

The single terms result using suitable quadrature rules in

$$
\begin{aligned}
\eta_{h,pu}^m &= -\frac{1}{2}\left[\left(b_1\left(\dot{\tilde{v}}_{kh}, \Pi_{2h}^{(0,2)}\tilde{\bar{u}}_{kh}\right)\right)_m + \left(a_1\left(\tilde{u}_{kh};\tilde{\theta}_{kh}\right)\left(\Pi_{2h}^{(0,2)}\tilde{\bar{u}}_{kh}\right)\right)_m - \left(l_1\left(\Pi_{2h}^{(0,2)}\tilde{\bar{u}}_{kh}\right)\right)_m\right] \\
&= -\frac{1}{2}b_1\left(\tilde{v}_{kh}^m - \tilde{v}_{kh}^{m-1}, \Pi_{2h}^{(2)}\tilde{\bar{u}}_{kh}^m\right) - \frac{k_m}{4}a_1\left(\tilde{u}_{kh}^m;\tilde{\theta}_{kh}^m\right)\left(\Pi_{2h}^{(2)}\tilde{\bar{u}}_{kh}^m\right) \\
&\quad -\frac{k_m}{4}a_1\left(\tilde{u}_{kh}^{m-1};\tilde{\theta}_{kh}^{m-1}\right)\left(\Pi_{2h}^{(2)}\tilde{\bar{u}}_{kh}^m\right) + \frac{k_m}{4}\left[l_1^m\left(\Pi_{2h}^{(2)}\tilde{\bar{u}}_{kh}^m\right) + l_1^{m-1}\left(\Pi_{2h}^{(2)}\tilde{\bar{u}}_{kh}^m\right)\right],
\end{aligned}
$$

$$
\begin{aligned}
\eta_{h,pv}^m &= -\frac{1}{2}\left(b_1\left(\dot{\tilde{u}}_{kh} - \tilde{v}_{kh}, \Pi_{2h}^{(0,2)}\tilde{\bar{v}}_{kh}\right)\right)_m \\
&= -\frac{1}{2}b_1\left(\tilde{u}_{kh}^m - \tilde{u}_{kh}^{m-1}, \Pi_{2h}^{(2)}\tilde{\bar{v}}_{kh}^m\right) + \frac{k_m}{4}b_1\left(\tilde{v}_{kh}^m + \tilde{v}_{kh}^{m-1}, \Pi_{2h}^{(2)}\tilde{\bar{v}}_{kh}^m\right),
\end{aligned}
$$

$$
\begin{aligned}
\eta^m_{h,p\theta} &= -\frac{1}{2}\left[\left(b_2\left(\dot{\tilde{\theta}}_{kh},\Pi^{(0,2)}_{2h}\tilde{\bar{\theta}}_{kh}\right)\right)_m+\left(a_2\left(\tilde{\theta}_{kh};\tilde{u}_{kh}\right)\left(\Pi^{(0,2)}_{2h}\tilde{\bar{\theta}}_{kh}\right)\right)_m-\left(l_2\left(\Pi^{(0,2)}_{2h}\tilde{\bar{\theta}}_{kh}\right)\right)_m\right]\\
&= -\frac{1}{2}b_2\left(\tilde{\theta}^m_{kh}-\tilde{\theta}^{m-1}_{kh},\Pi^{(2)}_{2h}\tilde{\bar{\theta}}^m_{kh}\right)-\frac{k_m}{4}a_2\left(\tilde{\theta}^m_{kh};\tilde{u}^m_{kh}\right)\left(\Pi^{(2)}_{2h}\tilde{\bar{\theta}}^m_{kh}\right)\\
&\quad -\frac{k_m}{4}a_2\left(\tilde{\theta}^{m-1}_{kh};\tilde{u}^{m-1}_{kh}\right)\left(\Pi^{(2)}_{2h}\tilde{\bar{\theta}}^m_{kh}\right)+\frac{k_m}{4}\left[l^m_2\left(\Pi^{(2)}_{2h}\tilde{\bar{\theta}}^m_{kh}\right)+l^{m-1}_2\left(\Pi^{(2)}_{2h}\tilde{\bar{\theta}}^m_{kh}\right)\right],
\end{aligned}
$$

$$
\begin{aligned}
\eta^m_{h,d\bar{u}} &= \frac{1}{2}\int_{I_m}J'_{1,u}\left(\tilde{w}_{kh}\right)\left(\Pi^{(1,2)}_{2h}\tilde{u}_{kh}\right)\,dt-\frac{1}{2}\left(a'_{1,u}\left(\tilde{u}_{kh};\tilde{\theta}_{kh}\right)\left(\Pi^{(1,2)}_{2h}\tilde{u}_{kh},\tilde{\bar{u}}_{kh}\right)\right)_m\\
&\quad -\frac{1}{2}\left(a'_{2,u}\left(\tilde{\theta}_{kh};\tilde{u}_{kh}\right)\left(\Pi^{(1,2)}_{2h}\tilde{u}_{kh},\tilde{\bar{\theta}}_{kh}\right)\right)_m+\frac{1}{2}b_1\left(\left[\tilde{\bar{v}}_{kh}\right]_m,\Pi^{(2)}_{2h}\tilde{u}^m_{kh}\right)\\
&= \frac{k_m}{4}\left[J'_{1,u}\left(\tilde{w}^m_{kh}\right)\left(\Pi^{(2)}_{2h}\tilde{u}^m_{kh}\right)+J'_{1,u}\left(\tilde{w}^{m-1}_{kh}\right)\left(\Pi^{(2)}_{2h}\tilde{u}^{m-1}_{kh}\right)\right]+\frac{1}{2}b_1\left(\tilde{\bar{v}}^{m+1}_{kh}-\tilde{\bar{v}}^m_{kh},\Pi^{(2)}_{2h}\tilde{u}^m_{kh}\right)\\
&\quad -\frac{k_m}{4}\left[a'_{1,u}\left(\tilde{u}^m_{kh};\tilde{\theta}^m_{kh}\right)\left(\Pi^{(2)}_{2h}\tilde{u}^m_{kh},\tilde{\bar{u}}^m_{kh}\right)+a'_{1,u}\left(\tilde{u}^{m-1}_{kh};\tilde{\theta}^{m-1}_{kh}\right)\left(\Pi^{(2)}_{2h}\tilde{u}^{m-1}_{kh},\tilde{\bar{u}}^m_{kh}\right)\right]\\
&\quad -\frac{k_m}{4}\left[a'_{2,u}\left(\tilde{\theta}^m_{kh};\tilde{u}^m_{kh}\right)\left(\Pi^{(2)}_{2h}\tilde{u}^m_{kh},\tilde{\bar{\theta}}^m_{kh}\right)+a'_{2,u}\left(\tilde{\theta}^{m-1}_{kh};\tilde{u}^{m-1}_{kh}\right)\left(\Pi^{(2)}_{2h}\tilde{u}^{m-1}_{kh},\tilde{\bar{\theta}}^m_{kh}\right)\right],
\end{aligned}
$$

$$
\begin{aligned}
\eta^m_{h,d\bar{v}} &= \frac{1}{2}\int_{I_m}J'_{1,v}\left(\tilde{w}_{kh}\right)\left(\Pi^{(1,2)}_{2h}\tilde{v}_{kh}\right)\,dt\\
&\quad +\frac{1}{2}\left[\left(b_1\left(\Pi^{(1,2)}_{2h}\tilde{v}_{kh},\tilde{\bar{v}}_{kh}\right)\right)_m+b_1\left(\left[\tilde{\bar{u}}_{kh}\right]_m,\Pi^{(2)}_{2h}\tilde{v}^m_{kh}\right)\right]\\
&= \frac{k_m}{4}\left[J'_{1,v}\left(\tilde{w}^m_{kh}\right)\left(\Pi^{(2)}_{2h}\tilde{v}^m_{kh}\right)+J'_{1,v}\left(\tilde{w}^{m-1}_{kh}\right)\left(\Pi^{(2)}_{2h}\tilde{v}^{m-1}_{kh}\right)\right]\\
&\quad +\frac{k_m}{4}b_1\left(\Pi^{(2)}_{2h}\left(\tilde{v}^m_{kh}+\tilde{v}^{m-1}_{kh}\right),\tilde{\bar{v}}^m_{kh}\right)+\frac{1}{2}b_1\left(\tilde{\bar{u}}^{m+1}_{kh}-\tilde{\bar{u}}^m_{kh},\Pi^{(2)}_{2h}\tilde{v}^m_{kh}\right),
\end{aligned}
$$

$$
\begin{aligned}
\eta^m_{h,d\bar{\theta}} &= \frac{1}{2}\int_{I_m}J'_{1,\theta}\left(\tilde{w}_{kh}\right)\left(\Pi^{(1,2)}_{2h}\tilde{\theta}_{kh}\right)\,dt-\frac{1}{2}\left(a'_{1,\theta}\left(\tilde{u}_{kh};\tilde{\theta}_{kh}\right)\left(\Pi^{(1,2)}_{2h}\tilde{\theta}_{kh},\tilde{\bar{u}}_{kh}\right)\right)_m\\
&\quad -\frac{1}{2}\left(a'_{2,\theta}\left(\tilde{\theta}_{kh};\tilde{u}_{kh}\right)\left(\Pi^{(1,2)}_{2h}\tilde{\theta}_{kh},\tilde{\bar{\theta}}_{kh}\right)\right)_m+\frac{1}{2}b_2\left(\left[\tilde{\bar{\theta}}_{kh}\right]_m,\Pi^{(2)}_{2h}\tilde{\theta}^m_{kh}\right)\\
&= \frac{k_m}{4}\left[J'_{1,\theta}\left(\tilde{w}^m_{kh}\right)\left(\Pi^{(2)}_{2h}\tilde{\theta}^m_{kh}\right)+J'_{1,\theta}\left(\tilde{w}^{m-1}_{kh}\right)\left(\Pi^{(2)}_{2h}\tilde{\theta}^{m-1}_{kh}\right)\right]+\frac{1}{2}b_2\left(\tilde{\bar{\theta}}^{m+1}_{kh}-\tilde{\bar{\theta}}^m_{kh},\Pi^{(2)}_{2h}\tilde{\theta}^m_{kh}\right)\\
&\quad -\frac{k_m}{4}\left[a'_{1,\theta}\left(\tilde{u}^m_{kh};\tilde{\theta}^m_{kh}\right)\left(\Pi^{(2)}_{2h}\tilde{\theta}^m_{kh},\tilde{u}^m_{kh}\right)+a'_{1,\theta}\left(\tilde{u}^{m-1}_{kh};\tilde{\theta}^{m-1}_{kh}\right)\left(\Pi^{(2)}_{2h}\tilde{\theta}^{m-1}_{kh},\tilde{u}^m_{kh}\right)\right]\\
&\quad -\frac{k_m}{4}\left[a'_{2,\theta}\left(\tilde{\theta}^m_{kh};\tilde{u}^m_{kh}\right)\left(\Pi^{(2)}_{2h}\tilde{\theta}^m_{kh},\tilde{\bar{\theta}}^m_{kh}\right)+a'_{2,\theta}\left(\tilde{\theta}^{m-1}_{kh};\tilde{u}^{m-1}_{kh}\right)\left(\Pi^{(2)}_{2h}\tilde{\theta}^{m-1}_{kh},\tilde{\bar{\theta}}^m_{kh}\right)\right].
\end{aligned}
$$

In the last time step, we only have to modify the terms connected to the dual residual. We obtain

$$\begin{aligned}
\eta_{h,d\bar{u}}^M &= \frac{1}{2}\int_{I_M} J'_{1,u}\left(\tilde{w}_{kh}\right)\left(\Pi_{2h}^{(1,2)}\tilde{u}_{kh}\right)\,dt + \frac{1}{2}J'_{2,u}\left(\tilde{w}_{kh}^M\right)\left(\Pi_{2h}^{(2)}\tilde{u}_{kh}^M\right) - \frac{1}{2}b_1\left(\tilde{\tilde{v}}_{kh}^M, \Pi_{2h}^{(2)}\tilde{u}_{kh}^M\right)\\
&\quad -\frac{1}{2}\left(a'_{1,u}\left(\tilde{u}_{kh};\tilde{\theta}_{kh}\right)\left(\Pi_{2h}^{(1,2)}\tilde{u}_{kh},\tilde{\tilde{u}}_{kh}\right)\right)_M - \frac{1}{2}\left(a'_{2,u}\left(\tilde{\theta}_{kh};\tilde{u}_{kh}\right)\left(\Pi_{2h}^{(1,2)}\tilde{u}_{kh},\tilde{\tilde{\theta}}_{kh}\right)\right)_M\\
&= \frac{k_M}{4}\left[J'_u\left(\tilde{w}_{kh}^M\right)\left(\Pi_{2h}^{(2)}\tilde{u}_{kh}^M\right) + J'_u\left(\tilde{w}_{kh}^{M-1}\right)\left(\Pi_{2h}^{(2)}\tilde{u}_{kh}^{M-1}\right)\right]\\
&\quad +\frac{1}{2}J'_{2,u}\left(\tilde{w}_{kh}^M\right)\left(\Pi_{2h}^{(2)}\tilde{u}_{kh}^M\right) - \frac{1}{2}b_1\left(\tilde{\tilde{v}}_{kh}^M, \Pi_{2h}^{(2)}\tilde{u}_{kh}^M\right)\\
&\quad -\frac{k_M}{4}\left[a'_{1,u}\left(\tilde{u}_{kh}^M;\tilde{\theta}_{kh}^M\right)\left(\Pi_{2h}^{(2)}\tilde{u}_{kh}^M,\tilde{\tilde{u}}_{kh}^M\right) + a'_{1,u}\left(\tilde{u}_{kh}^{M-1};\tilde{\theta}_{kh}^{M-1}\right)\left(\Pi_{2h}^{(2)}\tilde{u}_{kh}^{M-1},\tilde{\tilde{u}}_{kh}^M\right)\right]\\
&\quad -\frac{k_M}{4}\left[a'_{2,u}\left(\tilde{\theta}_{kh}^M;\tilde{u}_{kh}^M\right)\left(\Pi_{2h}^{(2)}\tilde{u}_{kh}^M,\tilde{\tilde{\theta}}_{kh}^M\right) + a'_{2,u}\left(\tilde{\theta}_{kh}^{M-1};\tilde{u}_{kh}^{M-1}\right)\left(\Pi_{2h}^{(2)}\tilde{u}_{kh}^{M-1},\tilde{\tilde{\theta}}_{kh}^M\right)\right],
\end{aligned}$$

$$\begin{aligned}
\eta_{h,d\bar{v}}^M &= \frac{1}{2}\int_{I_M} J'_v\left(\tilde{w}_{kh}\right)\left(\Pi_{2h}^{(1,2)}\tilde{v}_{kh}\right)\,dt + \frac{1}{2}J'_{2,v}\left(\tilde{w}_{kh}^M\right)\left(\Pi_{2h}^{(2)}\tilde{v}_{kh}^M\right)\\
&\quad +\frac{1}{2}\left(b_1\left(\Pi_{2h}^{(1,2)}\tilde{v}_{kh},\tilde{\tilde{v}}_{kh}\right)\right)_M - \frac{1}{2}b_1\left(\tilde{\tilde{u}}_{kh}^M, \Pi_{2h}^{(2)}\tilde{v}_{kh}^M\right)\\
&= \frac{k_M}{4}\left[J'_{1,v}\left(\tilde{w}_{kh}^M\right)\left(\Pi_{2h}^{(2)}\tilde{v}_{kh}^M\right) + J'_{1,v}\left(\tilde{w}_{kh}^{M-1}\right)\left(\Pi_{2h}^{(2)}\tilde{v}_{kh}^{M-1}\right)\right] + \frac{1}{2}J'_{2,v}\left(\tilde{w}_{kh}^M\right)\left(\Pi_{2h}^{(2)}\tilde{v}_{kh}^M\right)\\
&\quad +\frac{k_M}{4}b_1\left(\Pi_{2h}^{(2)}\left(\tilde{v}_{kh}^M + \tilde{v}_{kh}^{M-1}\right),\tilde{\tilde{v}}_{kh}^M\right) - \frac{1}{2}b_1\left(\tilde{\tilde{u}}_{kh}^M, \Pi_{2h}^{(2)}\tilde{v}_{kh}^M\right),
\end{aligned}$$

$$\begin{aligned}
\eta_{h,d\bar{\theta}}^M &= \frac{1}{2}\int_{I_M} J'_{1,\theta}\left(\tilde{w}_{kh}\right)\left(\Pi_{2h}^{(1,2)}\tilde{\theta}_{kh}\right)\,dt + \frac{1}{2}J'_{2,\theta}\left(\tilde{w}_{kh}^M\right)\left(\Pi_{2h}^{(2)}\tilde{\theta}_{kh}^M\right) - \frac{1}{2}b_2\left(\tilde{\tilde{\theta}}_{kh}^M, \Pi_{2h}^{(2)}\tilde{\theta}_{kh}^M\right)\\
&\quad -\frac{1}{2}\left(a'_{1,\theta}\left(\tilde{u}_{kh};\tilde{\theta}_{kh}\right)\left(\Pi_{2h}^{(1,2)}\tilde{\theta}_{kh},\tilde{\tilde{u}}_{kh}\right)\right)_M - \frac{1}{2}\left(a'_{2,\theta}\left(\tilde{\theta}_{kh};\tilde{u}_{kh}\right)\left(\Pi_{2h}^{(1,2)}\tilde{\theta}_{kh},\tilde{\tilde{\theta}}_{kh}\right)\right)_M\\
&= \frac{k_M}{4}\left[J'_{1,\theta}\left(\tilde{w}_{kh}^M\right)\left(\Pi_{2h}^{(2)}\tilde{\theta}_{kh}^M\right) + J'_{1,\theta}\left(\tilde{w}_{kh}^{M-1}\right)\left(\Pi_{2h}^{(2)}\tilde{\theta}_{kh}^{M-1}\right)\right]\\
&\quad +\frac{1}{2}J'_{2,\theta}\left(\tilde{w}_{kh}^M\right)\left(\Pi_{2h}^{(2)}\tilde{\theta}_{kh}^M\right) - \frac{1}{2}b_2\left(\tilde{\tilde{\theta}}_{kh}^M, \Pi_{2h}^{(2)}\tilde{\theta}_{kh}^M\right)\\
&\quad -\frac{k_M}{4}\left[a'_{1,\theta}\left(\tilde{u}_{kh}^M;\tilde{\theta}_{kh}^M\right)\left(\Pi_{2h}^{(2)}\tilde{\theta}_{kh}^M,\tilde{\tilde{u}}_{kh}^M\right) + a'_{1,\theta}\left(\tilde{u}_{kh}^{M-1};\tilde{\theta}_{kh}^{M-1}\right)\left(\Pi_{2h}^{(2)}\tilde{\theta}_{kh}^{M-1},\tilde{\tilde{u}}_{kh}^M\right)\right]\\
&\quad -\frac{k_M}{4}\left[a'_{2,\theta}\left(\tilde{\theta}_{kh}^M;\tilde{u}_{kh}^M\right)\left(\Pi_{2h}^{(2)}\tilde{\theta}_{kh}^M,\tilde{\tilde{\theta}}_{kh}^M\right) + a'_{2,\theta}\left(\tilde{\theta}_{kh}^{M-1};\tilde{u}_{kh}^{M-1}\right)\left(\Pi_{2h}^{(2)}\tilde{\theta}_{kh}^{M-1},\tilde{\tilde{\theta}}_{kh}^M\right)\right].
\end{aligned}$$

C.3 Numerical error estimate

In this section, we give the single terms of the numerical error estimator η_{it}. In the first time step, we obtain

$$\begin{aligned}
\eta_{\mathrm{it}}^0 &= -b_1\left(\tilde{u}_{kh}^0 - u_s, \tilde{\tilde{v}}_{kh}^0\right) - b_1\left(\tilde{v}_{kh}^0 - v_s, \tilde{\tilde{u}}_{kh}^0\right) - b_2\left(\tilde{\theta}_{kh}^0 - \theta_s, \tilde{\tilde{\theta}}_{kh}^0\right)\\
&\quad +b_1\left(\tilde{\tilde{u}}_{kh}^1 - \tilde{\tilde{u}}_{kh}^0, \tilde{v}_{kh}^0\right) + b_1\left(\tilde{\tilde{v}}_{kh}^1 - \tilde{\tilde{v}}_{kh}^0, \tilde{u}_{kh}^0\right) + b_2\left(\tilde{\tilde{\theta}}_{kh}^1 - \tilde{\tilde{\theta}}_{kh}^0, \tilde{\theta}_{kh}^0\right)
\end{aligned}$$

For a time step $0 < m \leq M$, it holds

$$\eta_{\mathrm{it}}^m = \left[A\left(\tilde{w}_{kh}\right)\left(\tilde{z}_{kh}\right)\right]_m =: \left[\eta_{\mathrm{it},u}^m + \eta_{\mathrm{it},v}^m + \eta_{\mathrm{it},\theta}^m\right].$$

The single terms result using suitable quadrature rules in

$$\begin{aligned}
\eta_{\mathrm{it},u}^m &= \left(b_1\left(\dot{\tilde{v}}_{kh},\tilde{\tilde{u}}_{kh}\right)\right)_m + \left(a_1\left(\tilde{u}_{kh};\tilde{\theta}_{kh}\right)\left(\tilde{\tilde{u}}_{kh}\right)\right)_m - \left(l_1\left(\tilde{\tilde{u}}_{kh}\right)\right)_m \\
&= b_1\left(\tilde{v}_{kh}^m - \tilde{v}_{kh}^{m-1},\tilde{\tilde{u}}_{kh}^m\right) + \frac{k_m}{2}a_1\left(\tilde{u}_{kh}^m;\tilde{\theta}_{kh}^m\right)\left(\tilde{\tilde{u}}_{kh}^m\right) \\
&\quad + \frac{k_m}{2}a_1\left(\tilde{u}_{kh}^{m-1};\tilde{\theta}_{kh}^{m-1}\right)\left(\tilde{\tilde{u}}_{kh}^m\right) + \frac{k_m}{2}\left[l_1^m\left(\tilde{\tilde{u}}_{kh}^m\right) + l_1^{m-1}\left(\tilde{\tilde{u}}_{kh}^m\right)\right],
\end{aligned}$$

$$\begin{aligned}
\eta_{\mathrm{it},v}^m &= \left(b_1\left(\dot{\tilde{u}}_{kh} - \tilde{v}_{kh},\tilde{\tilde{v}}_{kh}\right)\right)_m \\
&= b_1\left(\tilde{u}_{kh}^m - \tilde{u}_{kh}^{m-1},\tilde{\tilde{v}}_{kh}^m\right) - \frac{k_m}{2}b_1\left(\tilde{v}_{kh}^m + \tilde{v}_{kh}^{m-1},\tilde{\tilde{v}}_{kh}^m\right),
\end{aligned}$$

$$\begin{aligned}
\eta_{\mathrm{it},\theta}^m &= \left(b_2\left(\dot{\tilde{\theta}}_{kh},\tilde{\tilde{\theta}}_{kh}\right)\right)_m + \left(a_2\left(\tilde{\theta}_{kh};\tilde{u}_{kh}\right)\left(\tilde{\tilde{\theta}}_{kh}\right)\right)_m - \left(l_2\left(\tilde{\tilde{\theta}}_{kh}\right)\right)_m \\
&= b_2\left(\tilde{\theta}_{kh}^m - \tilde{\theta}_{kh}^{m-1},\tilde{\tilde{\theta}}_{kh}^m\right) + \frac{k_m}{2}a_2\left(\tilde{\theta}_{kh}^m;\tilde{u}_{kh}^m\right)\left(\tilde{\tilde{\theta}}_{kh}^m\right) \\
&\quad + \frac{k_m}{2}a_2\left(\tilde{\theta}_{kh}^{m-1};\tilde{u}_{kh}^{m-1}\right)\left(\tilde{\tilde{\theta}}_{kh}^m\right) + \frac{k_m}{2}\left[l_2^m\left(\tilde{\tilde{\theta}}_{kh}^m\right) + l_2^{m-1}\left(\tilde{\tilde{\theta}}_{kh}^m\right)\right].
\end{aligned}$$

D Adaptive solution algorithm for the dynamic mesh approach

Algorithm 11. Set the number of maximum iterations of the staggered solution scheme MAX and the stopping tolerance TOL, a stopping criterion, an initial spatial mesh $\mathbb{I}_h$, an initial temporal mesh $\mathbb{T}_k^0$ with M^0 time steps, a safety factor $c_f \in (0,1)$, a equilibration constant $c_e > 1$, $l = 0$, and $\mathbb{M}_h^l = (\mathbb{I}_h)_{0\le m\le M^0}$.

1. Solve the primal problem by the time stepping scheme given in Section 9 using MAX and TOL. Save $\tilde{w}_{kh}^l$.
2. Solve the dual problem by the time stepping scheme outline in Section 10 using MAX and TOL. Save $\tilde{z}_{kh}^l$.
3. Evaluate the error estimator $\eta + \eta^N$ and calculate the error indicators as outlined in Section 5.
4. If the stopping criterion is fulfilled, then set $w_{kh}^\star = w_{kh}^l$ and STOP.
5. If $\left|\eta^{N,l}\right| \ge c_f\left|\eta^l\right|$ set $l \leftarrow l+1$ and go to 1.
6. If $\left|\eta_h^{n,l}\right| \ge c_e\left|\eta_k^{i,l}\right|$ perform only spatial refinement, if $\left|\eta_k^{i,l}\right| \ge c_e\left|\eta_h^{n,l}\right|$ perform only temporal refinement, otherwise refine both.
7. If only temporal refinement, then set $\tilde{\mathbb{M}}_h^{l+1} = \mathbb{M}_h^l$ and go to 12.
8. Use the optimal mesh strategy to determine $\Theta_{h,r}^{DM,l} \subset \Theta_h^{DM,l}$, i. e. the spatial mesh cells for refinement.
9. Refine $\mathbb{M}_h^l$ according to $\Theta_{h,r}^{DM,l}$ ensuring the path structure and that only single hanging nodes in space occur. Call the result $\bar{\mathbb{M}}_h^{l+1}$.

10. Regularize the mesh sequence $\bar{\mathbb{M}}_h^{l+1}$ in time leading to $\tilde{\mathbb{M}}_h^{l+1}$.
11. If only spatial refinement, then set $\mathbb{M}_h^{l+1} = \tilde{\mathbb{M}}_h^{l+1}$ and $\mathbb{T}_k^{l+1} = \mathbb{T}_k^l$. Go to 14.
12. Use the optimal mesh strategy to determine $\Theta_{k,r}^l \subset \Theta_k^l$, i. e. the temporal mesh cells for refinement.
13. Refine the temporal mesh $\mathbb{T}_k^l$ and modify the spatial mesh sequence $\tilde{\mathbb{M}}_h^{l+1}$ according to $\Theta_{k,r}^l$. Call the results $\mathbb{T}_k^{l+1}$ and $\mathbb{M}_h^{l+1}$.
14. Set $l \leftarrow l + 1$ and go to 1.